

เทพโพรไฟลิงของมัลติเลเซอร์ฟิล์ม
โดยอุปกรณ์รับรู้โดมอนต์ไมโครเอทีอาร์ชนิดใหม่ที่มีปลายแหลม



นางสาววิภาภรณ์ อัครชรรยง

สถาบันวิทยบริการ

วิทยานิพนธ์นี้เป็นส่วนหนึ่งของการศึกษาตามหลักสูตรปริญญาวิทยาศาสตรมหาบัณฑิต
สาขาวิชาปิโตรเคมีและวิทยาศาสตร์พอลิเมอร์

คณะวิทยาศาสตร์ จุฬาลงกรณ์มหาวิทยาลัย

ปีการศึกษา 2548

ISBN 974-53-2710-7

ลิขสิทธิ์ของจุฬาลงกรณ์มหาวิทยาลัย

DEPTH PROFILING OF MULTILAYER FILMS
BY NOVEL SHARP TIP DIAMOND μ ATR SENSOR



Miss Wipaporn Akkarayanyong

A Thesis Submitted in Partial Fulfillment of the Requirements
for the Degree of Master of Science Program in Petrochemistry and Polymer Science

Faculty of Science


Chulalongkorn University

Academic Year 2005

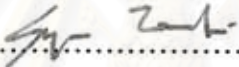
ISBN 974-53-2710-7

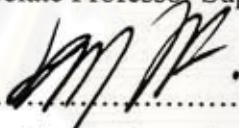
Thesis Title Depth profiling of multilayer films by novel sharp tip diamond
 μ ATR sensor
By Miss Wipaporn Akkarayanyong
Field of Study Petrochemistry and Polymer Science
Thesis Advisor Associate Professor Sanong Ekgasit, Ph.D.
Thesis Co-advisor Associate Professor Chuchaat Thammacharoen

Accepted by the Faculty of Science, Chulalongkorn University in Partial
Fulfillment of the Requirements for the Master's Degree

.....Dean of the Faculty of Science
(Professor Piamsak Menasveta, Ph.D.)

THESIS COMMITTEE

.....Chairman
(Associate Professor Supawan Tantayanon, Ph.D.)

.....Thesis Advisor
(Associate Professor Sanong Ekgasit, Ph.D.)

Chuchaat Thammacharoen.....Thesis Co-advisor
(Associate Professor Chuchaat Thammacharoen)

Warinthorn Chavasiri.....Member
(Assistant Professor Warinthorn Chavasiri, Ph.D.)

Vp. Hoven.....Member
(Assistant Professor Voravee P. Hoven, Ph.D.)

วิทยานิพนธ์ อัครขรรจร: เคฟ โพร ไฟลิ่งของมัลติเลเยอร์ฟิล์ม โดยอุปกรณ์รับรู้ไคมอนด์ไมโครเอทีอาร์ชนิดใหม่ที่มีปลายแหลม (DEPTH PROFILING OF MULTILAYER FILMS BY NOVEL SHARP TIP DIAMOND μ ATR SENSOR) อ. ที่ปรึกษา: รศ. ดร. สนอง เอกสิทธิ์, อ. ที่ปรึกษาร่วม: รศ. ชูชาติ ธรรมเจริญ, 70 หน้า. ISBN 974-53-2710-7.

อุปกรณ์รับรู้ไคมอนด์ไมโครเอทีอาร์ชนิดใหม่ใช้เพชรที่เจียรระไนแล้วเป็นไออาร์อี โดยอุปกรณ์นี้ถูกนำมาใช้งานร่วมกับกล้องจุลทรรศน์อินฟราเรดเพื่อศึกษาสมบัติที่เปลี่ยนแปลงตามความลึกของมัลติเลเยอร์ฟิล์ม เทคนิคนี้สามารถตรวจวิเคราะห์ได้โดยไม่ต้องเตรียมสารตัวอย่างและใช้เวลาในการวิเคราะห์น้อย เนื่องจากเพชรที่ใช้เป็นไออาร์อีมีความแข็งแรงสูงและมีปลายแหลมจึงสามารถนำมาใช้ศึกษาสมบัติที่เปลี่ยนแปลงตามความลึกของตัวอย่างของแข็งได้ การศึกษาองค์ประกอบทางเคมีของสารที่เปลี่ยนแปลงตามความลึกของมัลติเลเยอร์ฟิล์มสามารถตรวจวิเคราะห์ได้โดยการให้แรงกดเพื่อเพิ่มความลึกของปลายเพชรที่เข้าไปในสารตัวอย่างขณะเดียวกันก็ควบคุมอะเพอเจอร์ของกล้องจุลทรรศน์อินฟราเรดให้คงที่ หรือเปลี่ยนแปลงขนาดของอะเพอเจอร์แต่ควบคุมให้ความลึกของปลายเพชรที่เข้าไปในสารตัวอย่างให้คงที่ สเปกตรัมที่ได้จากการวิเคราะห์โดยใช้อุปกรณ์รับรู้ที่ทำด้วยเพชรนี้ถูกนำมาเปรียบเทียบกับการวิเคราะห์ด้วยอุปกรณ์เพิ่มเติมเอทีอาร์ที่มีขายเชิงพาณิชย์ เนื่องจากการตรวจวิเคราะห์โดยใช้อุปกรณ์เพิ่มเติมเอทีอาร์ที่มีขายเชิงพาณิชย์ใช้ศึกษาสมบัติที่เปลี่ยนแปลงตามความลึกของสารได้ในระดับไม่กี่ไมโครเมตร ดังนั้นเอทีอาร์สเปกตรัมที่ได้จึงแสดงให้เห็นเฉพาะข้อมูลเชิงพื้นผิวของมัลติเลเยอร์ฟิล์มเท่านั้น ในขณะที่สเปกตรัมที่ได้จากการตรวจวิเคราะห์ด้วยอุปกรณ์รับรู้ที่ทำด้วยเพชรแสดงให้เห็นถึงการเปลี่ยนแปลงขององค์ประกอบทางเคมีของสารที่ระดับความลึกต่างๆ ของมัลติเลเยอร์ฟิล์มอย่างชัดเจน

สถาบันวิทยบริการ จุฬาลงกรณ์มหาวิทยาลัย

สาขาวิชา... ปิโตรเคมีและวิทยาศาสตร์พอลิเมอร์... ลายมือชื่อนิสิต... อัครขรรจร
ปีการศึกษา... 2548... ลายมือชื่ออาจารย์ที่ปรึกษา...
ลายมือชื่ออาจารย์ที่ปรึกษาร่วม...

4772475023 : MAJOR PETROCHEMISTRY AND POLYMER SCIENCE

KEY WORDS: MULTILAYER FILMS / DIAMOND μ ATR SENSOR / DIAMOND IRE /ATR FT-IR SPECTROSCOPY / ATR FT-IR MICROSPECTROSCOPY

WIPAPORN AKKARAYANYONG: DEPTH PROFILING OF MULTILAYER FILMS BY NOVEL SHARP TIP DIAMOND μ ATR SENSOR. THESIS ADVISOR: ASSOC. PROF. SANONG EKGASIT, PH.D., THESIS CO-ADVISOR: ASSOC. PROF. CHUCHAAT THAMMACHAROEN, 70 pp. ISBN 974-53-2710-7

The novel diamond μ ATR sensor for ATR FT-IR spectral acquisition using infrared microscope with a gem quality faceted diamond as an internal reflection element (IRE) was employed for the depth profiling of multilayered films. This technique does not require additional sample preparation and has short analysis time. Due to the inherent hardness and sharp-tip, the diamond IRE can be employed for probing depth dependent properties of solid materials. The depth dependent composition of the multilayered film can be collected by varying the diamond penetration under a constant aperture of infrared microscope or by varying the aperture under a constant diamond penetration. The observed spectra were compared to those obtained via the commercial ATR accessory. The ATR spectra acquired by the commercial ATR accessory show the surface information of multilayered film since the probing depth was limited to few micrometers from the interface. The spectra acquired by the diamond μ ATR sensor clearly indicate the depth dependent chemical information exhibiting different chemical species of multilayered film.

สถาบันวิทยบริการ
จุฬาลงกรณ์มหาวิทยาลัย

Field of study.....Petrochemistry and polymer science..... Student's signature.....*วิภากรณ์ อัครายุทธ*
Academic year.....2005..... Advisor's signature.....*สม.ท.*
Co-advisor's signature.....*Chuchaat Thammacharoen*

ACKNOWLEDGEMENTS

I would like to express my sincere gratitude to Associate Professor Dr. Supawan Tantayanon, Assistant Professor Dr. Warinthorn Chavasiri, and Assistant Professor Dr. Voravee P. Hoven for the insightful suggestions and contribution as thesis committee.

Gratefully thanks to Associate Professor Chuchaat Thammacharoen, my thesis co-advisor, and Dr. Pimthong Thongnopkun for the invaluable guidance, comments, and suggestions.

Finally, this thesis would not have been successfully completed without the excellent advice from my thesis advisor, Associate Professor Dr. Sanong Ekgasit, who always provides me the useful guidance, suggestion, encouragement, and understanding and also patiently practices my technical skill during the whole research.

Warmest thanks to my friends and colleagues at the Sensor Research Unit for the everlasting friendship and spiritual supports throughout the time of study.

Above all, I am profoundly grateful to my wonderful parents and the endearing family for their patient love, perpetual encouragement, and overwhelming support.

สถาบันวิทยบริการ
จุฬาลงกรณ์มหาวิทยาลัย

CONTENTS

	Pages
ABSTRACT IN THAI.....	iv
ABSTRACT IN ENGLISH.....	v
ACKNOWLEDGEMENTS.....	vi
CONTENTS.....	vii
LIST OF FIGURES.....	x
LIST OF TABLES.....	xiv
LIST OF ABBREVIATIONS.....	xv
LIST OF SYMBOLS.....	xvi
CHAPTER I INTRODUCTION.....	1
1.1 Multilayered Films Characterization.....	1
1.2 Fourier Transform Infrared (FT-IR) Spectroscopy.....	1
1.2.1 ATR FT-IR Spectroscopy.....	2
1.2.2 ATR FT-IR Microspectroscopy.....	3
1.3 Scope of the Research.....	5
1.4 Objectives of the Research.....	5
CHAPTER II THEORETICAL BACKGROUND.....	6
2.1 Basic Concept of Spectroscopy.....	6
2.2 Attenuated Total Reflection Fourier Transform Infrared Spectroscopy	8
2.2.1 Principles of Light Reflection and Refraction.....	8
2.2.2 Internal Reflection Element (IRE).....	11
2.2.3 ATR Spectral Intensity.....	12
2.2.4 Depth Profiling Using ATR FT-IR Spectroscopy.....	14
2.2.5 Limitation of ATR FT-IR Spectroscopy.....	17
2.3 ATR FT-IR Microscopy.....	17
2.3.1 Infrared Microscope.....	17

	Pages
2.3.2 Novel ATR FT-IR Microscopy using a Gem Quality Diamond IRE.....	19
2.3.3 Principle of Light That Entering the Diamond IRE	21
CHAPTER III EXPERIMENTAL SECTION.....	23
3.1 Materials and Equipments.....	23
3.1.1 Samples.....	23
3.1.2 Instruments.....	23
3.2 Default Spectral Acquisition.....	24
3.3 Homemade diamond μ ATR accessory.....	25
3.4 Surface Characterization by ATR FT-IR Spectroscopy.....	27
3.4.1 Experimental Procedure for the Conventional ATR Accessory....	27
3.4.2 Experimental Procedure for Diamond μ ATR Sensor	28
3.5 Depth Profiling by ATR FT-IR Spectroscopy.....	28
3.5.1 Experimental Procedure for the Conventional ATR Accessory.....	28
3.5.2 Experimental Procedure for Diamond μ ATR Sensor	29
CHAPTER IV RESULTS AND DISCUSSION.....	32
4.1 Parameters Affecting Novel Diamond μ ATR Measurement.....	32
4.1.1 Characteristic Absorption of the Diamond IRE	32
4.1.2 Diamond Arrangement	34
4.1.3 Variation of Apertures	36
4.2 Surface Characterization of Homogeneous Sample.....	38
4.2.1 Mineral Oil.....	38
4.2.2 Poly(vinyl chloride).....	39
4.3 Depth Profiling of Homogeneous samples	39
4.3.1 Mineral Oil.....	40
4.3.1.1 Conventional ATR technique.....	40
4.3.1.2 Diamond μ ATR technique.....	41

	Pages
4.3.2 Poly(vinyl chloride).....	42
4.3.2.1 Conventional ATR technique.....	42
4.3.2.2 Diamond μ ATR technique.....	43
4.4 Surface Characterization of Heterogeneous Sample	46
4.4.1 OPP/PE.....	46
4.4.2 Teflon/Polyimide/Teflon	46
4.5 Depth Profiling of Homogeneous samples	47
4.5.1 OPP/PE.....	47
4.5.1.1 Conventional ATR technique.....	47
4.5.1.2 Diamond μ ATR technique.....	49
4.5.2 Teflon/Polyimide/Teflon.....	53
4.5.2.1 Conventional ATR technique.....	53
4.5.2.2 Diamond μ ATR technique.....	55
CHAPTER V CONCLUSIONS.....	60
REFERENCES.....	61
APPENDICES.....	63
CURRICULUM VITAE.....	70

LIST OF FIGURES

	Pages
2.1 Propagation of a linearly polarized electromagnetic wave in space. Electric (E) and magnetic (H) vectors are always perpendicular to each other and to the direction of propagation.....	6
2.2 Interactions of light with matter.....	7
2.3 Reflection and refraction of a plane wave at a dielectric based on Snell's Law.....	9
2.4 Condition under which total internal reflection occurs. Light travels from an optically denser medium and impinges at the surface of the optically rarer medium ($n_1 > n_2$) with angle of incidence equal the critical angle.....	10
2.5 Selected IRE configurations commonly used in ATR experimental setups: (a) Single reflection variable-angle hemispherical crystal and (b) Multiple reflection single-pass crystal.....	12
2.6 The MSEF at various experimental condition (A, A') and its decay characteristic (B, B'). The simulation parameters are $n_0 = 4.00$ for Ge, $n_0 = 2.40$ for ZnSe, $\nu = 1000 \text{ cm}^{-1}$, $n_1(\nu) = 1.50$, $k_1(\nu) = 0.0, 0.1, 0.2, 0.3, 0.4$ and 0.5 , respectively.....	14
2.7 Relationship between the penetration depth and wavenumber for Ge crystal ($n = 4.0$) at different angle of incidence.....	16
2.8 Relationship between penetration depth and wavenumber for ZnSe crystal ($n = 2.4$) at different angle of incidence.....	16
2.9 Optical diagram for infrared microscope.....	18
2.10 Path of the infrared radiation in through an ATR objective of infrared microscope.....	19
2.11 Transflectance spectra of round brilliant cut natural diamond.....	20
2.12 A schematic drawing of a round brilliant cut diamond	21

2.13	Ray tracing of the coupled radiations within the faceted diamond. Angles of reflections and refractions defined with respect to the direction normal are summarized.....	22
3.1	Composition of the homemade diamond μ ATR accessory: the diamond probing head, the adjustable reflection plane and complete set of homemade accessory.....	26
3.2	The homemade diamond μ ATR accessory mounted onto the infrared microscope	27
3.3	Schematic illustration of depth profiling using a hemispherical ZnSe IRE, variable angles of incidence	29
3.4	Schematic illustration of the depth-dependent measurement using a diamond IRE. The spectra were collected as varying aperture under a constant diamond penetration	30
3.5	Schematic illustration of the depth-dependent measurement using a diamond IRE. The spectra were collected as the diamond penetrates deeper into the solid sample under a constant aperture	31
4.1	Transflectance spectra of round brilliant cut natural diamonds with different concentrations of nitrogen impurities.....	33
4.2	FT-IR spectra of PVC acquired by diamond μ ATR sensor: (A) spectrum of diamond IRE, (B) spectrum of PVC and diamond IRE, (C) spectrum of PVC when the contributions of diamond IRE was subtracted and (D) ATR spectrum of PVC obtained via conventional ZnSe IRE with 45° angle of incidence.....	34
4.3	Transflectance spectra of a round brilliant cut diamond under difference diamond orientations: 0° , 45° , 90° , 180° and 270° with respect to the reference position. The inset shows overlaid spectra in the one-phonon region.....	35

4.4	Normalized ATR spectra of a mineral oil on the diamond IRE under difference diamond rotation. The diamond was rotated at 0°, 45°, 90°, 180° and 270° with respect to the reference position. The inset shows the superimposition of the ATR spectra of the mineral oil in the C-H stretching region.....	36
4.5	Normalized transmittance spectra of a round brilliant cut diamond under varying the aperture sizes of infrared microscope.....	37
4.6	ATR spectra of mineral oil acquired by two sampling techniques: (A) conventional ATR using 45° ZnSe IRE and (B) diamond μ ATR sensor.....	38
4.7	ATR spectra of PVC acquired by two sampling techniques: (A) conventional ATR using 45° ZnSe IRE and (B) diamond μ ATR sensor.....	39
4.8	Normalized ATR spectra of mineral oil acquired by conventional ATR using ZnSe IRE. The angle of incidence was varied from 45° to 60° with a 5° interval	40
4.9	Normalized ATR spectra of mineral oil: (A) spectrum acquired by conventional ATR and (B) depth profiling by the diamond μ ATR sensor, the aperture of microscope were set at 500x500, 400x400, 300x300, 200x200 and 100x100 μm^2	41
4.10	Normalized ATR spectra of PVC acquired by conventional ATR using ZnSe IRE. The angle of incidence was varied from 45° to 60° with a 5° interval.....	42
4.11	Normalized ATR spectra of PVC: (A) spectrum acquired by conventional ATR and (B) depth profiling by increasing diamond penetration under a constant aperture of the diamond μ ATR sensor.....	44
4.12	Normalized ATR spectra of PVC: (A) spectrum acquired by conventional ATR and (B) depth profiling by variable the aperture under a constant diamond penetration of the diamond μ ATR sensor.....	45

4.13	ATR spectra of both side of OPP/PE bi-layered film: (A) OPP side and (B) PE side. The spectra were acquired by conventional ATR using 45° ZnSe IRE and the diamond μ ATR sensor.....	46
4.14	ATR spectra of individual layers of Teflon/Polyimide/Teflon multilayered film acquired by two sampling techniques: conventional ATR using 45° ZnSe IRE and diamond μ ATR sensor.....	47
4.15	Normalized ATR spectra of OPP/PE bi-layered film acquired by conventional ATR using ZnSe IRE. The angle of incidence was varied from 45° to 60° with a 5° for each interval	49
4.16	Normalized ATR spectra of OPP/PE: (A) spectra of OPP acquired by conventional ATR, (B) depth profiling of OPP/PE by increasing diamond penetration under a constant aperture of the diamond μ ATR sensor, F_1 denote the applied force that $F_1 < F_2 < F_3 < F_4 < F_5$ and (C) spectrum of PE acquired by conventional ATR.....	51
4.17	Normalized ATR spectra of OPP/PE: (A) spectrum of OPP acquired by conventional ATR, (B) depth profiling of OPP/PE by increasing aperture under a constant diamond penetration of the diamond μ ATR sensor and (C) spectrum of PE acquired by conventional ATR.....	53
4.18	Normalized ATR spectra of Teflon/Polyimide/Teflon acquired by conventional ATR using ZnSe IRE. The angle of incidence was varied from 45° to 60° with a 5° interval.....	54
4.19	Normalized ATR spectra of multilayered film: (A) spectra of Teflon (outside), polyimide, and Teflon (inside) acquired by conventional ATR and (B) depth profiling of Teflon/Polyimide/Teflon by increasing diamond penetration under a constant aperture of the diamond μ ATR sensor, F_1 denote the applied force that $F_1 < F_2 < F_3 < F_4 < F_5$	56
4.20	ATR spectra of multilayered film: (A) spectra of each layers of Teflon/Polyimide/Teflon acquired by conventional ATR and (B) depth profiling of Teflon/Polyimide/Teflon by increasing aperture under a constant diamond penetration of the diamond μ ATR sensor.....	58

LIST OF TABLES

	Pages
2.1 Properties of materials used for internal reflection elements.....	11



สถาบันวิทยบริการ
จุฬาลงกรณ์มหาวิทยาลัย

LIST OF ABBREVIATIONS

ATR	: attenuated total reflection
FT-IR	: Fourier transform infrared
Ge	: germanium
IR	: infrared
IRE	: internal reflection element
MCT	: mercury cadmium telluride
MSEF	: mean square electric field
μm	: micrometer
OPP	: oriented polypropylene
PE	: polyethylene
PVC	: poly(vinyl chloride)
ZnSe	: zinc selenide
N/A	: not available



สถาบันวิทยบริการ
จุฬาลงกรณ์มหาวิทยาลัย

LIST OF SYMBOLS

A	: absorbance
d_p	: penetration depth
I	: intensity
n	: refractive index
R	: reflectance
ν	: wavenumber
μ	: micro
θ	: angle of incidence
θ_c	: critical angle



สถาบันวิทยบริการ
จุฬาลงกรณ์มหาวิทยาลัย

CHAPTER I

INTRODUCTION

1.1 Multilayered Films Characterization

Multilayered films have been an important development in packaging technology. They are designed to provide enhanced properties which are suitable for each specific application. The driving force behind the development has been focusing on wearing and corrosive resistance, chemical resistance, labeling, and extended coating lifetime. It has been revealed that the surface structure of multi-component polymer is different from that of the bulk. To gain an insight understanding of the specific chemical composition and structure of the surface and bulk regions, the surface characterization and depth profiling analysis has been an important technique in identifying the chemical composition [1].

There are varieties of sampling techniques of specifically application to surface and depth profiling studies such as X-ray diffraction [1-2], or secondary ion mass spectroscopy (SIMS) [1]. However, these analytical techniques give us the information only about the distribution of elements and not about the changes in chemical bonding or chemical structure of organic materials. Fourier transform infrared (FT-IR) spectroscopy is particularly important because of the rich information content of the chemical composition and molecular structure [3]. This technique can be applied to study a layered material in order to determine the chemical nature of different species.

1.2 Fourier Transform Infrared (FT-IR) Spectroscopy

FT-IR spectroscopy offers the materials scientist a relatively direct probe of the molecular structure, particularly when it is applied to surface and depth profiling analysis. Surface characterization techniques are required to probe the surface and interface regions. A good surface characterization technique should have the

following properties: nondestructive, quick and easy sampling, high accuracy and high resolution with quantitative analysis. The technique should be sensitive to the changes in the sample such as compositional changes. However, there is no technique that can satisfy all these requirements. Some techniques offer exceptionally high sensitivity but their applicability is severely limited by high costs, limited availability, destructive nature, difficulty in sample preparation, and extremely testing conditions. The user must sacrifice part of the sampling requirements, sample preparation, and acquired information when choosing a surface characterization technique.

In the past, the traditional transmission technique was employed for multi-component analysis [4-5]. The technique involves passing the infrared radiation through the sample and detecting a portion of the radiation via the transmission process. The sample must be separated into individual layers or sliced subdivision of the sample by processes such as microtoming and analyze each of the constituent part of the structure variation within the sample. Transmission mode is destructive sampling technique and needs sample preparation. Within FT-IR spectroscopy, very few techniques are available for nondestructive analysis and advanced to surface and depth profile analysis such as attenuated total reflection Fourier transform infrared (ATR FT-IR) spectroscopy [6-7].

1.2.1 ATR FT-IR Spectroscopy

ATR FT-IR spectroscopy has been used in a wide variety of application including nondestructive analysis, quantitative analysis [8], qualitative analysis [9], surface characterization [4, 10], and depth profiling [11-15]. In the ATR technique, the sample is placed against an internal reflection element (IRE). The IRE is made of material with high refractive index such as germanium (Ge), silicon (Si) or zinc selenide (ZnSe). The total internal reflection occurs at the interface as the angle of incidence greater than the critical angle is utilized. Depth profiling can be performed by the use of various IRE from different materials having different refractive indices [11] or varying the angles of incidence [11-15].

In an ATR experiment, optical contact between the IRE and the sample plays an important role on obtaining a good spectral quality. From physical characteristic of sample, liquid sample always wet the surface of the IRE. As a result, a perfect contact between the sample and IRE is always achieved. The solid sample, on the other hand, rarely has a good contact with the IRE especially the sample with rough surface. Although the solid sample with mirror-flat surface is employed, the optical contact between the sample and IRE is difficult to obtain due to dust and local irregularity of the surface. When the optical contact is not achieved, there is an air gap between the sample and IRE. If an air gap is large enough, an ATR spectrum cannot be observed. In the general practice, applying pressure to a solid sample against the IRE is the technique for improving the contact between the sample and IRE. This technique is not always applicable since the excessive force may damage the IRE and/or cause a rapid deterioration of the IRE especially when a soft IRE is employed. To overcome these limitations, diamond has been used as an infrared window in high-pressure cells [16] and for special ATR applications. The benefits of diamond are strength, hardness, chemical resistance, and transparency throughout most of the mid-infrared region. Solid sample with an irregular surface requires a method of providing intimate contact with the IRE. In the case of the diamond IRE, the small physical size of the diamond and its intrinsic hardness can help to obtain the optimal sampling condition via an applied pressure.

1.2.2 ATR FT-IR Microspectroscopy

Infrared microanalysis was developed in the early 1980s [5, 17, 18]. The FT-IR microspectroscopy is defined as the coupling of a microscope to an infrared spectrometer. Infrared microscope has been developed in order to reveal the small fractions of sample in both transmission and reflection modes. For ATR measurement, the specialized objective for internal reflection microspectroscopy provides the optics for viewing the sample and a high refractive index material. This element is constituted by a hemispheric prism mounted on the IR objective that called ATR objective. This new class of objective has solved some of the problems encountered in analysis at a macroscopic level of the conventional ATR technique.

The multi-component analysis is performed following three modes: a survey mode for viewing and selecting the sampling area to analysis, a contact mode to bring the sample in contact with the ATR objective and an ATR mode for infrared analysis. Different types of ATR objective are available such as ZnSe, Si and Ge crystals are employed to depth profiling analysis [9, 19]. Due to the low mechanical strength of material, the pressure application is constrained onto the IRE.

In 1995, a new micro-ATR accessory was introduced (the DurasamplIR from SenIR Technologies, USA) [5, 20]. In its standard form, this accessory features a diamond IRE sampling surface. All the practical benefits of diamond are retained: its strength and chemical inertness, and good optical performance with minimum interference in the region of the diamond absorption. This arrangement is made practically by a unique combination of a small, thin diamond element placed on top of a larger optical element which made from a material of comparable refractive index, usually zinc selenide. The second, larger element acts as a mechanical support and as a focusing device for the infrared radiation entering and exiting the diamond IRE. However, on a larger optical element placed by thin diamond IRE there is the limitation of hardness. If high pressure is applied, it will break or crack. Moreover, the commercial accessory is expensive.

From the limitation of commercial diamond micro-ATR, the novel diamond μ ATR sensor was developed [21]. The novel ATR microscope for spectral acquisition using a gem quality round brilliant cut diamond as IRE was introduced. The advantage of the homemade diamond μ ATR sensor is to reduce the cost. In addition, the diamond μ ATR sensor requires short acquisition time while sample preparation is not necessary. By employing the diamond IRE with sharp-tip configuration, surface, bulk, and/or depth-dependent information of solid materials can be acquired. With a diamond μ ATR sensor accessory, user is provided with one of the most reproducible sampling methods available for sampling with optical contact problem in hard and rigid materials, rough surface, irregular shape samples, and sample with small sampling area. As long as the sample is under moderately applied pressure, good optical contact is always achieved at the diamond tip.

1.3 The Objective of This Research

The objective of this research is to exploit the novel diamond μ ATR sensor for surface characterization and to apply for depth profiling analysis of multilayered films.

1.4 Scope of the Research

1. To develop the novel diamond μ ATR sensor for surface characterization and depth profiling of multilayered films.
2. To compare the ATR spectral observation by the diamond μ ATR sensor with the conventional ATR using ZnSe IRE



สถาบันวิทยบริการ
จุฬาลงกรณ์มหาวิทยาลัย

CHAPTER II

THEORETICAL BACKGROUND

2.1 Basic Concepts of Spectroscopy

Spectroscopy is the study of the interaction of electromagnetic radiation with matter [6]. When the electromagnetic radiation impinges on the surface of a matter, interactions between the incident beam and the molecules will alter the incident radiation. The incident beam can be reflected, scattered, transmitted, or absorbed by the matter. These modifications give information about the molecular or physical properties of the matter. A spectroscopic experiment allows the detection of reflected, scattered, transmitted, or absorbed light.

While a matter and a detector are defined by specific chemical and physical properties, light needs further consideration. Light is an electromagnetic wave. According to classical wave theory, the electric field vector (E) and the magnetic field vector (H) of a radiation are oscillating periodically in space, as shown in Figure 2.1. The electric and magnetic vector components and the direction of propagation are perpendicular to each others [6].

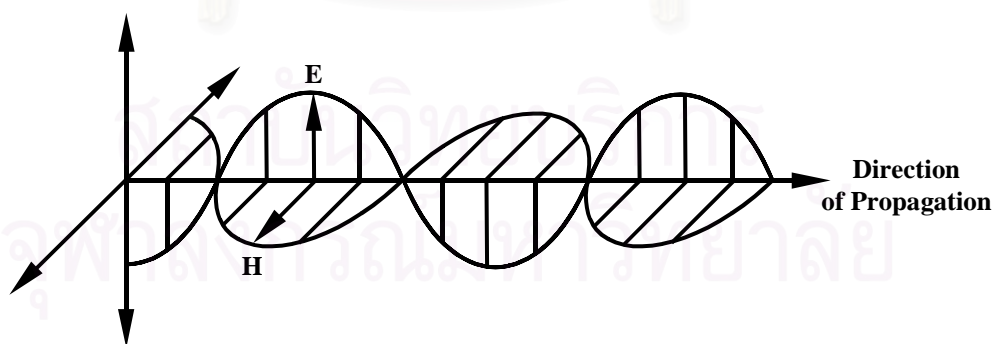


Figure 2.1 Propagation of a linearly polarized electromagnetic wave in space. Electric (E) and magnetic (H) vectors are always perpendicular to each other and to the direction of propagation.

When an electromagnetic radiation impinges on a matter, rays of the incident beam may be reflected, scattered, transmitted, or absorbed that depending on the experimental arrangement. The total amount of incident energy is the sum of reflected, scattered, transmitted, and absorbed light. A schematic illustration for an interaction between light and matter is illustrated in Figure 2.2. This process can be expressed by the following relationship [6]:

$$I_0 = I_R + I_S + I_T + I_A \quad (2.1)$$

where I_0 is the intensity of the incident radiation and I_R , I_S , and I_T are the reflected, scattered, and transmitted radiations, respectively. I_A is the radiation absorbed by matter. The intensity of each radiation depends on the intensity and wavelength of the incident radiation, the optical properties of the specimen, the concentrations of species, and the geometry of the experimental setup.

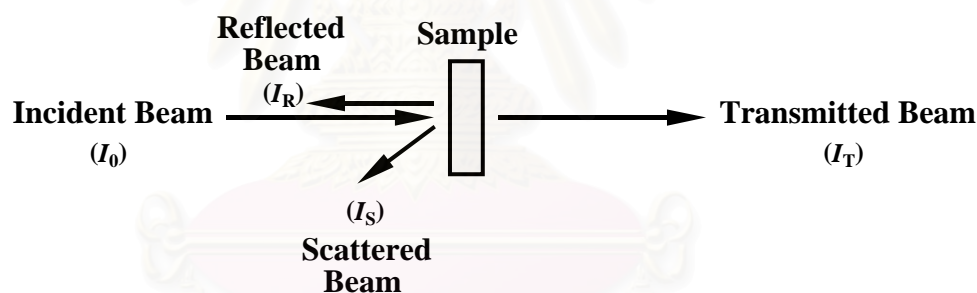


Figure 2.2 Interactions of light with matter.

Consider the electromagnetic radiation when a sample is inserted between a light source and a detector. The sample absorbs a fraction of the incident radiation. In order to measure the region and amount of light being absorbed by the sample, we need to measure the ratio of the sample attenuated (I_T) and nonattenuated (I_0) intensities of the radiation. The ratio is proportional to the transmittance of the sample. This relationship can be quantitatively related to the chemical composition of the sample by the Beer-Lambert law as [6]:

$$I / I_0 = e^{-A(\bar{\nu})} = e^{-c_2 \varepsilon(\bar{\nu}) l} \quad (2.2)$$

where $A(\bar{\nu})$ is the sample absorbance at a given wavenumber $\bar{\nu}$, c_2 is the concentration of the absorbing functional group, $\varepsilon(\bar{\nu})$ is the wavenumber-dependent absorption coefficient, and l is the film thickness for the IR beam at a normal incidence to the sample surface.

The simple transmission technique implicates passing the infrared radiation through the sample and detecting a portion of the radiation that is transmitted. This technique may provide a significant amount of information concerning molecular structures and their properties. Nevertheless, transmission mode is not applicable to surface analysis. If one requires gaining an insight understanding of the surface properties such as chemical compositions, molecular orientation, and chemical reaction, a surface sensitive technique is required. Attenuated total reflection (ATR) FT-IR spectroscopy is a good candidate for that purpose. It is not only a technique that provides the information, which directly associated to chemical composition of the sample, but also a surface sensitive sampling technique.

2.2 Attenuated Total Reflection Fourier Transform Infrared (ATR FT-IR) Spectroscopy

ATR FT-IR spectroscopy is a characterization technique based on an internal reflection principle. The major factors driving this developed technique are reduced sample preparation, the ease-of-use of internal reflection spectroscopy attachments. In experimental, a sample need only be placed in optical contact with the surface of the IRE to record its ATR spectra.

2.2.1 Principles of Light Reflection and Refraction

Reflection of light or radiant energy is the abrupt change in the direction of propagation when the radiation is incident on an interface. An optical interface is created whenever there is a discrete change in optical properties; namely the

refractive index and/or absorption index. When electromagnetic radiation strikes a boundary between two media with different refractive indices, refraction and reflection occur. The law that governs the reflection process requires that the angle of incidence be equal to the angle of reflection. In this case, reflection is specular. If electromagnetic radiation passes from one medium to another that has a different refractive index, a sudden change of beam direction is detected because of the difference in propagation velocity through two media. If light propagates through a medium with refractive index n_1 and enters a medium with refractive index n_2 (see Figure 2.3), the light path will change, the extent of refraction is given by the following relationship [6]:

$$\frac{\sin \alpha_1}{\sin \alpha_2} = \frac{n_2(\bar{\nu})}{n_1(\bar{\nu})} \quad (2.3)$$

where α_1 and α_2 are the angle of incidence and refraction, respectively.

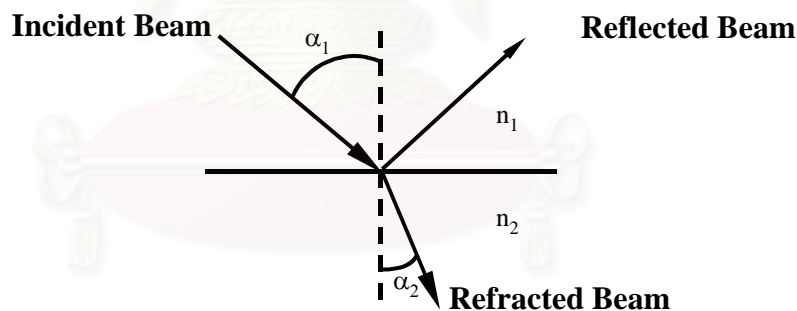


Figure 2.3 Reflection and refraction of a plane wave at a dielectric based on Snell's Law.

Total internal reflection occurs when light (or radiant energy) traveling through a medium of high refractive index is incident on the interface with a lower index (i.e., $n_1 > n_2$) with an incident angle greater than the critical angle. The critical angle can be derived from Snell's law and given by Equation 2.4 [6-7].

$$\theta_c = \sin^{-1}(n_2(\bar{\nu}) / n_1(\bar{\nu})). \quad (2.4)$$

According to Figure 2.4, when the angle of incidence equals the critical angle, θ_c , the refracted angle equals 90° . This implies that under a total internal reflection phenomenon there is no light from the optically denser medium travels across the interface into the optically rarer medium. If the rarer medium is nonabsorbing, then all incident radiation (*i.e.*, at angles greater than the critical angle) are internally reflected. If the rarer medium absorbs radiation at a specific wavelength, the intensity of the reflected radiation is reduced at that particular wavelength. In other words, the internal reflection is attenuated. This attenuation of the total reflection produces ATR spectra.

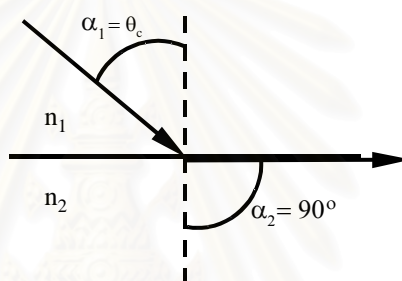


Figure 2.4 Condition under which total internal reflection occurs. Light travels from an optically denser medium and impinges at the surface of the optically rarer medium ($n_1 > n_2$) with angle of incidence equal the critical angle.

Total internal reflection spectroscopy is, therefore, the technique of recording the optical spectrum of a sample material that is in contact with an optically denser medium. The wavelength dependence of the reflectivity of this interface is measured by introducing light into the denser medium. In this technique the reflectivity is a measure of the interaction of the electric field with the material and the resulting spectrum is also a characteristic of the material.

2.2.2 Internal Reflection Element (IRE)

The internal reflection element (IRE) or ATR crystal must have a high reflective index and be transparent throughout the mid-infrared spectral region. The IRE must also withstand physical and chemical contact with samples. It is not too surprising that few materials meet these requirements. Listed in Table 2.1 are the optical and mechanical properties of infrared transmitting materials [5].

Table 2.1 Properties of materials used for internal reflection elements.

Material	Reflective index At 1000 cm^{-1}	Useful range (cm^{-1})	Maximum use T ($^{\circ}\text{C}$)	Hardness (kg mm^{-2})
Germanium	4.02	5,500-600	100	780
Silicon	3.42	8,300-660	300	1150
Zinc selenide	2.43	20,000-460	315	120
Diamond	2.417	45,000-~2,500, ~1650-200	550	8820

The IRE is used in internal reflection spectroscopy for establishing the conditions necessary to obtain internal reflection spectra of materials (Figure 2.5). Radiation propagates through the IRE by means of internal reflection. The sample material is placed into contact with the IRE. The ease of obtaining an internal reflection spectrum and the information obtained from the spectrum are determined by the characteristics of the IRE (*i.e.*, single or multiple reflections). A choice must be made in the working angle or range of angles of incidence, number of reflections, aperture, number of passes, surface preparation, and material from which it is made [7].

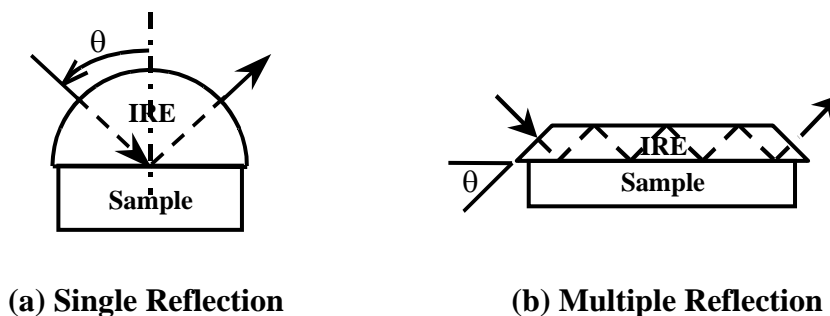


Figure 2.5 Selected IRE configurations commonly used in ATR experimental setups: (a) Single reflection variable-angle hemispherical crystal and (b) Multiple reflection single-pass crystal.

2.2.3 ATR Spectral Intensity

In an ATR configuration, a medium with a high refractive index is optically contacted with a medium with lower refractive index (*i.e.*, sample). The IRE is infrared transparent. The sample, on the other hand, is infrared absorbing and has a complex refractive index at frequency ν of $n_1(\nu) = n_1(\nu) + ik_1(\nu)$, where $n_1(\nu)$ and $k_1(\nu)$ are refractive index and absorption index, respectively. Incident light travels from the IRE and impinges the IRE-absorbing medium interface with an angle of incidence is greater than the critical angle, total internal reflection can occur.

Under non-absorbing conditions [*i.e.*, $k_1(\nu) = 0$], the incident light is totally reflected at the interface. Since no light travels across the interface and there is no reflection loss due to absorption [*i.e.*, reflectance $R(\theta, \nu) = 1$], this phenomenon is then called the total reflection phenomenon.

When a rarer medium is absorbing [*i.e.*, $k_1(\nu) > 0$], there is reflection loss due to absorbing by the material [*i.e.*, $R(\theta, \nu) < 1$]. This phenomenon is called the ATR phenomenon. Although no light travels across the boundary, there is a strong electric field at the interface region of the absorbing medium. Interaction between the electric field and the absorbing medium is the cause of reflection loss in ATR experiment. The magnitudes of the interaction between light and the sample can be

expressed in terms of absorbance. The absorbance depends on both the material properties (e.g., refractive index of the IRE and refractive index of the sample) and the experimental parameters (e.g., angle of incidence, frequency, and polarization of the incident beam). The relationship between absorbed and reflected intensity in an ATR spectrum is given by [15]:

$$A(\theta, \nu) = 1 - R(\theta, \nu) \quad (2.5)$$

where $A(\theta, \nu)$ and $R(\theta, \nu)$ are absorptance and reflectance, respectively. In general, absorptance in ATR can be expressed in terms of experimental parameters and material characteristic by the following expression [15, 22]:

$$A_l(\theta, \nu) = \frac{4\pi\nu}{n_0 \cos \theta} \int_0^\infty n_1(\nu) k_1(\nu) \langle E_{z,l}^2(\theta, \nu) \rangle dz \quad (2.6)$$

where $A(\theta, \nu)$ is absorptance and l indicates the polarization of the incident beam. $\langle E_{z,l}^2(\theta, \nu) \rangle$ is the mean square electric field (MSEF) at depth z , $n_1(\nu)$ and $k_1(\nu)$, respectively, are the refractive index and absorption index of the sample, and n_0 is the refractive index of the IRE.

The MSEF is a function of both experimental parameters and material characteristics. The relationship between the absorption strength and the material properties shown in equation 2.6 is nonlinear. In general, the MSEF is strongest at the IRE/sample interface. Its strength decreases exponentially as a function of depth. The strength and decay characteristic of the MSEF vary with the absorption strength are shown in Figure 2.6.

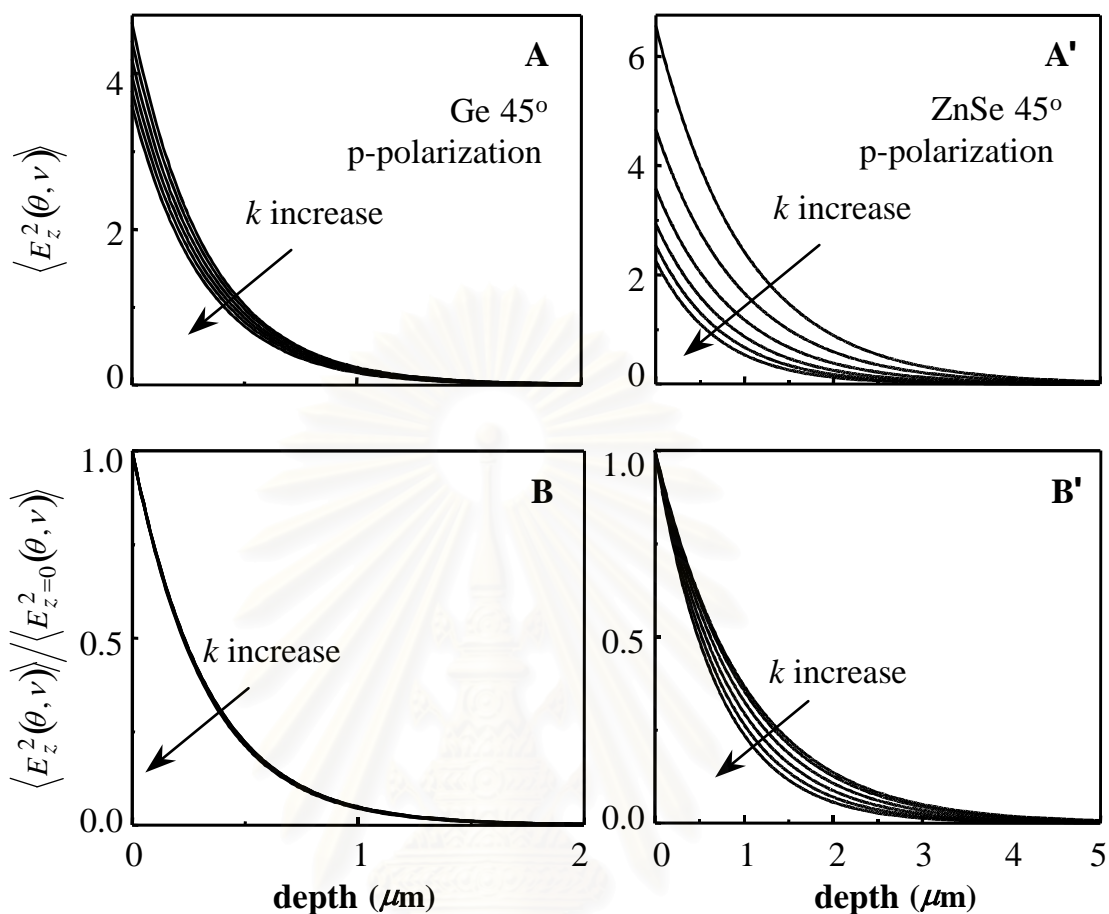


Figure 2.6 The MSEF at various experimental condition (A, A') and its decay characteristic (B, B'). The simulation parameters are $n_0 = 4.00$ for Ge, $n_0 = 2.40$ for ZnSe, $\nu = 1000 \text{ cm}^{-1}$, $n_1(\nu) = 1.50$, $k_1(\nu) = 0.0, 0.1, 0.2, 0.3, 0.4$ and 0.5 , respectively.

2.2.4 Depth Profiling Using ATR FT-IR Spectroscopy

ATR FT-IR spectroscopy has long been recognized as a surface characterization and depth profiling techniques. The main factor that makes ATR technique suitable for depth profiling application is the MSEF under total internal reflection condition. The MSEF strength is greatest at the interface between the IRE and the sample. It decays exponentially as a function of distance from the interface. The distance from the interface where the field strength decay to $1/e$ of that the interface is called penetration depth. Therefore, the ATR technique can be used to

obtain a degree of depth profile analysis by changing the penetration depth. The penetration depth is given in terms of material characterization and experimental parameters by [7]:

$$d_p = \frac{1}{2\pi\nu n_0 (\sin^2 \theta - (n_1/n_0)^2)^{1/2}} \quad (2.7)$$

where $d_p(\theta, \nu)$ is the penetration depth. The penetration depth also depends on experimental conditions and material characteristics.

According to equation 2.7, there are several important parameters that affect the observed spectrum and spectral qualities. One of them is the refractive index. At a fixed angle of incidence, the penetration depth is larger for better index matching (i.e., n_1 is similar to n_0). When an organic material (refractive index of 1.5) is placed in contact with a ZnSe IRE (refractive index of 2.4), the ratio of the refractive indices is $(n_1/n_0) = 0.625$. In contrary, when an organic material is in contact with a germanium IRE (refractive index of 4.0), the ratio of the refractive indices becomes 0.375. According to Figure 2.7 and 2.8, the penetration depth with ZnSe as the IRE is greater than that with Ge. It also indicates that the penetration depth depend largely on the frequency of the incident beam. As the frequency of the infrared light increases the penetration depth decreases. However in FT-IR practice, it is often convenient to express frequency in terms of wavenumber, the penetration depth decreases when wavenumber increases. This also leads to a decrease of relative band intensities in the ATR spectrum with increasing wavenumber. Furthermore, changing the angles of incident effects on the penetration depth. If the angle of incident is increased, the penetration depth will be decreased and the spectral intensity will be decreased. The greater penetration depth implies a greater distance from surface of the sample where chemical information can be observed by ATR technique.

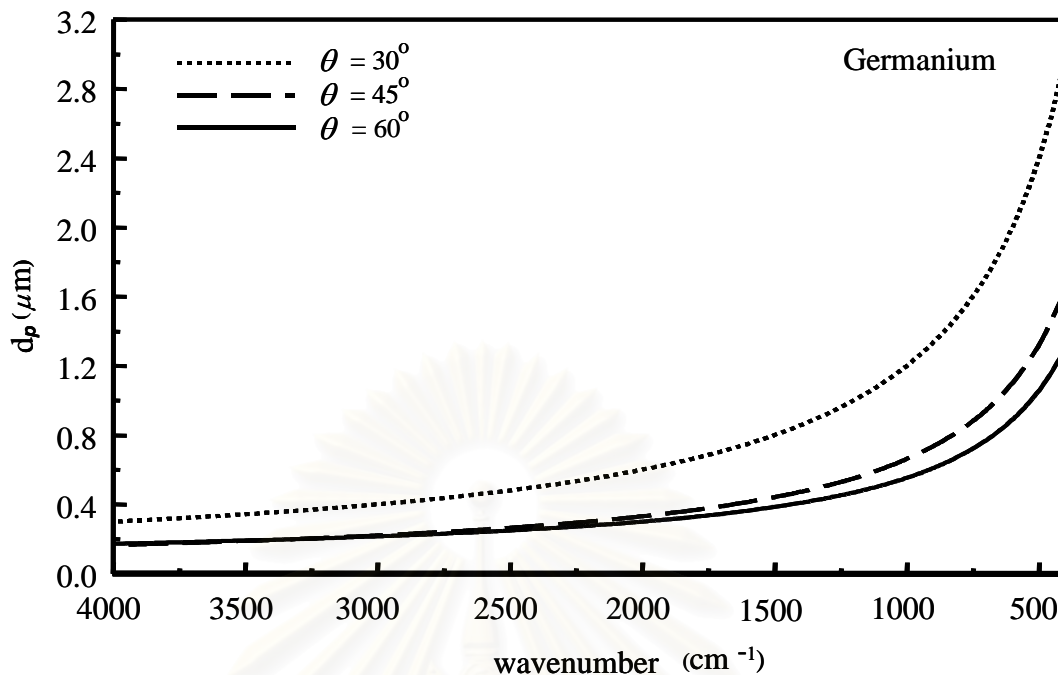


Figure 2.7 Relationship between the penetration depth and wavenumber for Ge crystal ($n = 4.0$) at different angle of incidence.

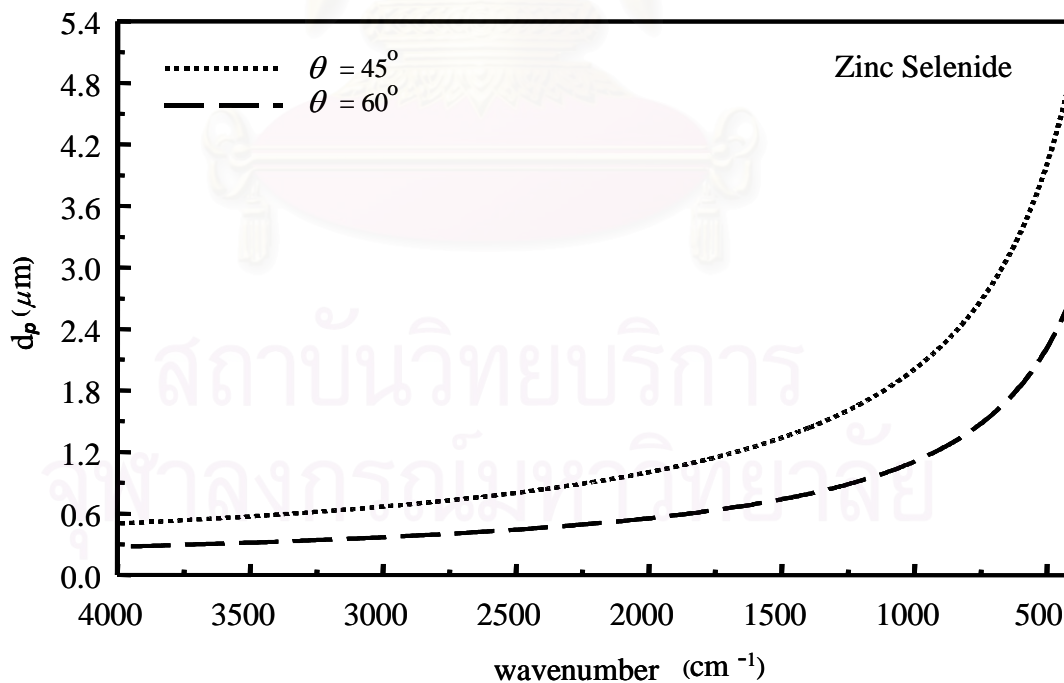


Figure 2.8 Relationship between penetration depth and wavenumber for ZnSe crystal ($n = 2.4$) at different angle of incidence.

The depth profiling by ATR FT-IR spectroscopy can be performed by using IRE of different refractive index, and/or by varying the angle of incidence of the infrared light in the IRE. Lower refractive index and smaller angle of incidence lead to increase the penetration depth.

2.2.5 Limitation of ATR FT-IR spectroscopy

ATR FT-IR spectroscopy is a surface sensitive technique. However, it has several limited applications. One of them is a contact between the sample and IRE [15, 22]. In order to obtain good ATR spectra, a very good contact between the sample and IRE is required. Liquid samples always have a perfect contact with IRE. The solid sample rarely has a good contact with the IRE especially the hard and rigid solid. When the system does not achieve an optical contact, there is always an air gap between the sample and the IRE. The larger is the air gap, the smaller is the observed spectral intensity. If an air gap is large enough the spectrum can not be obtained. To solve this problem, the high pressure is applied at the sample against the IRE. However, the IRE may be damaged by an excessive pressure. Another limitation for ATR FT-IR spectroscopy is the depth of penetration. Since the ATR spectra sensitive to physical phenomena in a few micrometers near the interface, spectral information at a greater depth cannot be obtained.

2.3 ATR FT-IR Microscopy

2.3.1 Infrared Microscope

FT-IR microscopy defines as the coupling of a microscope to an infrared spectrometer. This coupling allows one to focus infrared radiation onto the specimen, to collect transmitted or reflected infrared radiation from the sample by a detector [5, 17, 18]. The optical diagram of an infrared microscope is shown in Figure 2.9.

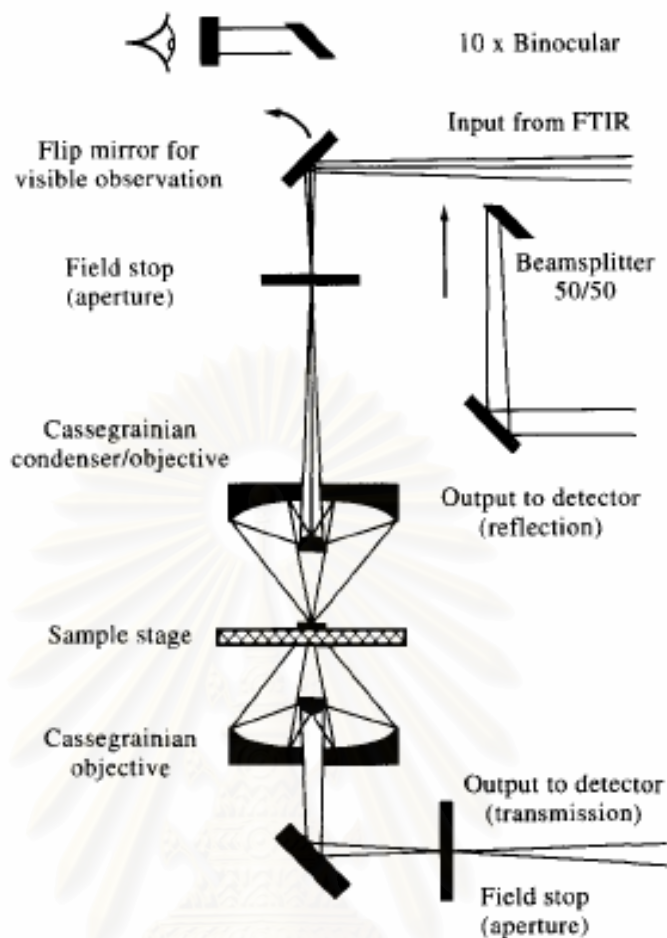


Figure 2.9 Optical diagram for infrared microscope.

Infrared microscope has been developed in order to reveal the small and fractions of layer samples that are beyond the capability of normal infrared spectrometer. Infrared microscope is generally designed with two paths from the sample to the detector; transmission and reflection. For transmission mode, the infrared light passes through the sample. The transmitted radiation is collected by second infrared objective and sends the radiation to the detector. Therefore, the sample must be very thin or compressible in order to allow the light to pass through. The technique may require more sample preparation. For reflection mode, the infrared light reflects off of the sample and passes back through the illuminating objective. An appropriate sample requires almost no sample preparation.

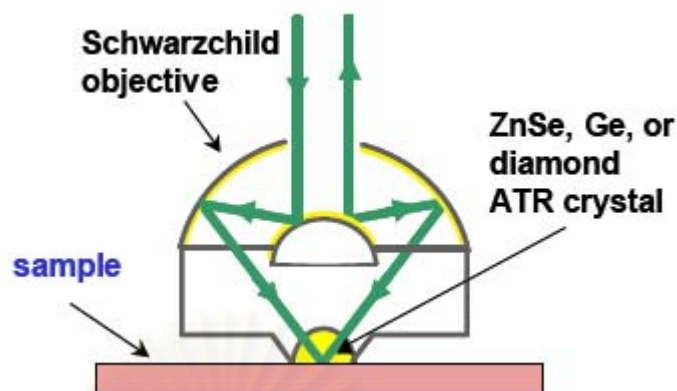


Figure 2.10 Path of the infrared radiation in through an ATR objective of infrared microscope.

ATR is one of the reflection modes which based on the phenomenon known as total internal reflection. As mentioned before in the general case, when radiation traveling in a medium of high refractive index strikes an interface with a lower refractive index material the radiation is partly reflected and partly refracted. A diagram of an ATR objective for an infrared microscope is shown in Figure 2.10. The high refractive index material is in the form of a hemisphere and the sample to be investigated is pressed against the flat surface of the hemisphere. Since the hemisphere is small, diamond becomes affordable as the high refractive index material.

2.3.2 Novel ATR FT-IR Microscopy using a Gem Quality Diamond IRE

Diamond is absorbing in the mid-infrared region (Figure 2.11). It has three major absorption bands, namely one-phonon ($1400\text{-}900\text{ cm}^{-1}$), two-phonon ($2650\text{-}1500\text{ cm}^{-1}$), and three-phonon ($3900\text{-}2650\text{ cm}^{-1}$) absorption [21, 23]. The absorption magnitude in the one-phonon region depends strongly on the concentration of nitrogen impurities. Diamond with high nitrogen content always shows over absorption in this region. The two-phonon region is indicated the specifically structure of diamond that always over absorbing in this region. The three-phonon region is associated with hydrogen impurity in the diamond structure.

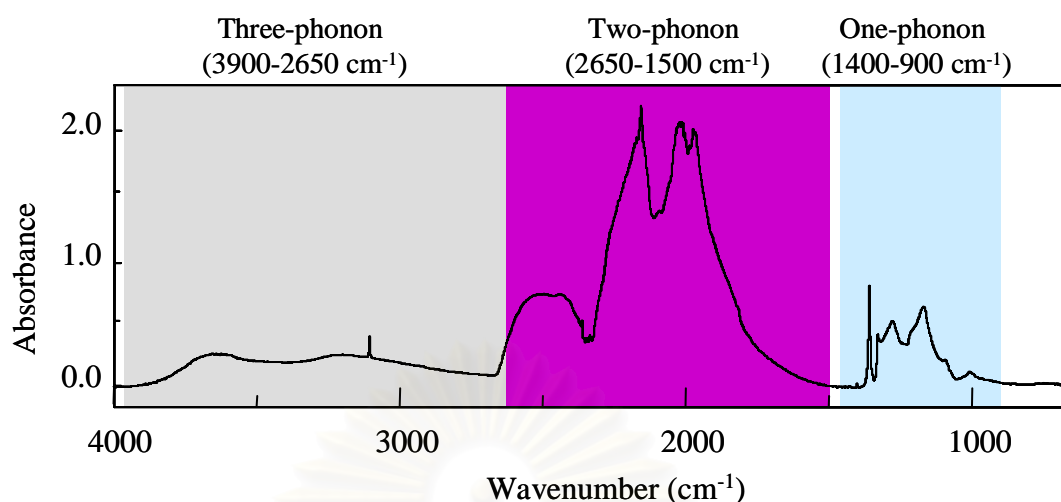


Figure 2.11 Transflectance spectra of round brilliant cut natural diamond.

In principle, a gem quality brilliant cut diamond was cut in such a proportion that the number of total internal reflection within the diamond is enhanced. To increase the number of total internal reflection, the cutting proportion of the diamond is carefully design with respect to its refractive index, size, shape, and carat weight. The number of reflection depends on the angle and positions that light enter the diamond. The greater the number of total internal reflections, the better is the fire and brilliance of the diamond. This phenomenon is due to the dispersion of light associated with its traveling distance and the total internal reflection inside diamond. A modern brilliant cut diamond consists of $57+1$ facets depending on the presence of the culet (Figure 2.12). Diamond can be employed as an IRE because its high refractive index ($n_{\text{diamond}} = 2.417$) is greater than that of sample ($n_{\text{organic}} = 1.5$). Total internal reflection at the diamond/sample interface is observed when radiation traveling inside the diamond impinges the interface with an angle greater than the critical angle. The critical angle (θ_C) is given in terms of the refractive index by $\theta_C = \sin^{-1} (n_{\text{sample}}/n_{\text{diamond}})$ and is equal 38.36 for the diamond/organic material interface [21].

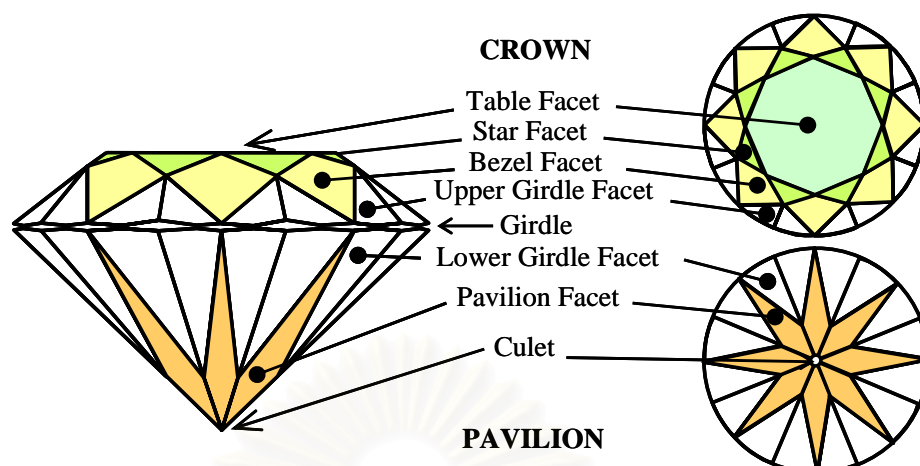


Figure 2.12 A schematic drawing of a round brilliant cut diamond.

2.3.3 Principle of Light that Entering the Diamond IRE

In order to collect ATR FT-IR spectra of a faceted diamond using an infrared microscope, the infrared radiation is coupled into and is collected from the table facet by the built-in 15X Cassegrainian objective, for the coupled radiation with a normal incidence to the table facet, the radiation totally reflects at the pavilion facet. Under the employed cut proportion (*i.e.*, a set of Tolkowsky's recommended proportion with pavilion angle of 41° and crown angle of 34° [21, 23]), the angles of reflection at the pavilion facet are 41° and 57° for the first and second reflections, respectively. The radiation reaches the diamond/air interface at the table facet with an angle of 16° and refracts into air with an angle of 41.77° . Due to the complex cut the surfaces of the faceted diamond, the coupled radiations that impinge the table facet with different angles and/or positions undergo different reflections inside the faceted diamond before emerging into air at any facets. According to the traveling path of the coupled radiation (Figure 2.13), the outgoing radiation from the table facet is defined as the transflected radiation. The evanescent field under total internal reflection at the pavilion facets can interact with a material attached to the diamond. By collecting the transreflectance spectrum, absorption of the material under ATR condition can be acquired [21].

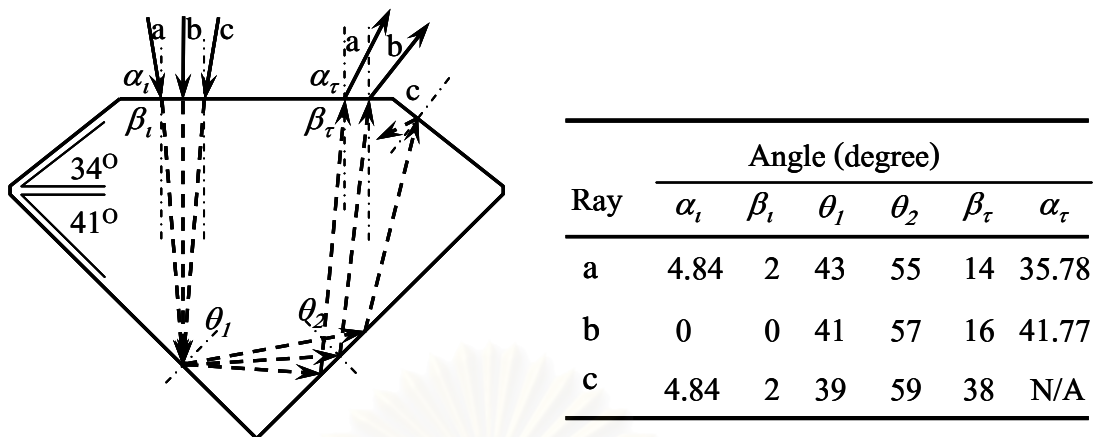


Figure 2.13 Ray tracing of the coupled radiations within the faceted diamond. Angles of reflections and refractions defined with respect to the direction normal are summarized.

CHAPTER III

EXPERIMENTAL SECTION

The novel diamond μ ATR sensor based on ATR principle was applied for surface characterization and depth profiling of isotropic and anisotropic samples. For comparison purpose, depth profiling study was divided into two procedures; (1) varying diamond penetration under constant aperture and (2) constant diamond penetration with variable aperture. The observed ATR spectra acquired by the novel diamond IRE will be compared to those acquired by a traditional ZnSe IRE.

3.1 Materials and Equipments

3.1.1. Samples

1. Homogeneous samples
 - 1.1 Mineral oil
 - 1.2 Poly(vinyl chloride) or PVC
2. Heterogeneous samples
 - 2.1 Oriented polypropylene coated on polyethylene (OPP/PE)
 - 2.2 Teflon/Polyimide/Teflon multilayered film

3.1.2 Instruments

1. Nicolet Magna 750 FT-IR spectrometer equipped with a mercury-cadmium-telluride (MCT) detector
2. NICPLANTM infrared microscope with 15X Cassegrain infrared objective and 10X glass objective
3. Variable-angle single-reflection attenuated total reflection accessory (The SeagullTM, Harrick Scientific, USA) with a hemispherical ZnSe IRE.

4. Homemade diamond μ ATR accessory equipped with a gem-quality round brilliant cut diamond IRE (0.1005 ct type IaB natural diamond)

3.2 Default Spectral Acquisition

Nicolet Magna 750 FT-IR Spectrometer

Instrumental Setup

Source	Standard Global TM Infrared Light Source
Detector	MCT
Beam splitter	Ge-coated KBr

Acquisition Parameters

Spectral resolution	4 cm ⁻¹
Number of scans	256 scans
Spectral format	Absorbance

Advanced Parameters

Zero filing	none
Apodization	Happ-Genzel
Phase correction	Mertz

NICPLAN Infrared Microscope

Instrumental Setup

Source	Standard Global TM Infrared Light Source
Detector	MCT
Beam splitter	Ge-coated KBr

Acquisition Parameters

Spectral resolution	4 cm ⁻¹
Number of scans	256 scans
Spectral format	Absorbance

Advanced Parameters

Zero filing	none
Apodization	Happ-Genzel

3.3 Homemade diamond μ ATR accessory

The homemade diamond μ ATR sensor accessory composes of two parts as shown in Figure 3.1. First component is probing head which designed for mounting the diamond IRE. It contains a sample holder whereby a solid sample can be brought into contact with the culet of the diamond IRE. Another component is the adjustable reflection plane. The three knobs setting on the corner of this plate (Figure 3.1) were employed for adjusting the table facet of the diamond IRE perpendicular to the incident radiation in order to obtain a high energy throughput.

The homemade accessory was placed onto the stage of NICPLANTM infrared microscope connected to the Nicolet Magna 750 FT-IR spectrometer, illustrated in Figure 3.2. The homemade accessory is capable of analyzing sample in transmittance mode. The incident infrared radiation from the infrared microscope is coupled onto the table facet of the diamond IRE. The amount of light is controlled by the aperture of the microscope. The infrared radiation was focused at the culet of the diamond IRE. The sample focus can be adjusted by the knobs of the homemade accessory and the stage of the microscope is adjusted in order to obtain high energy throughput.

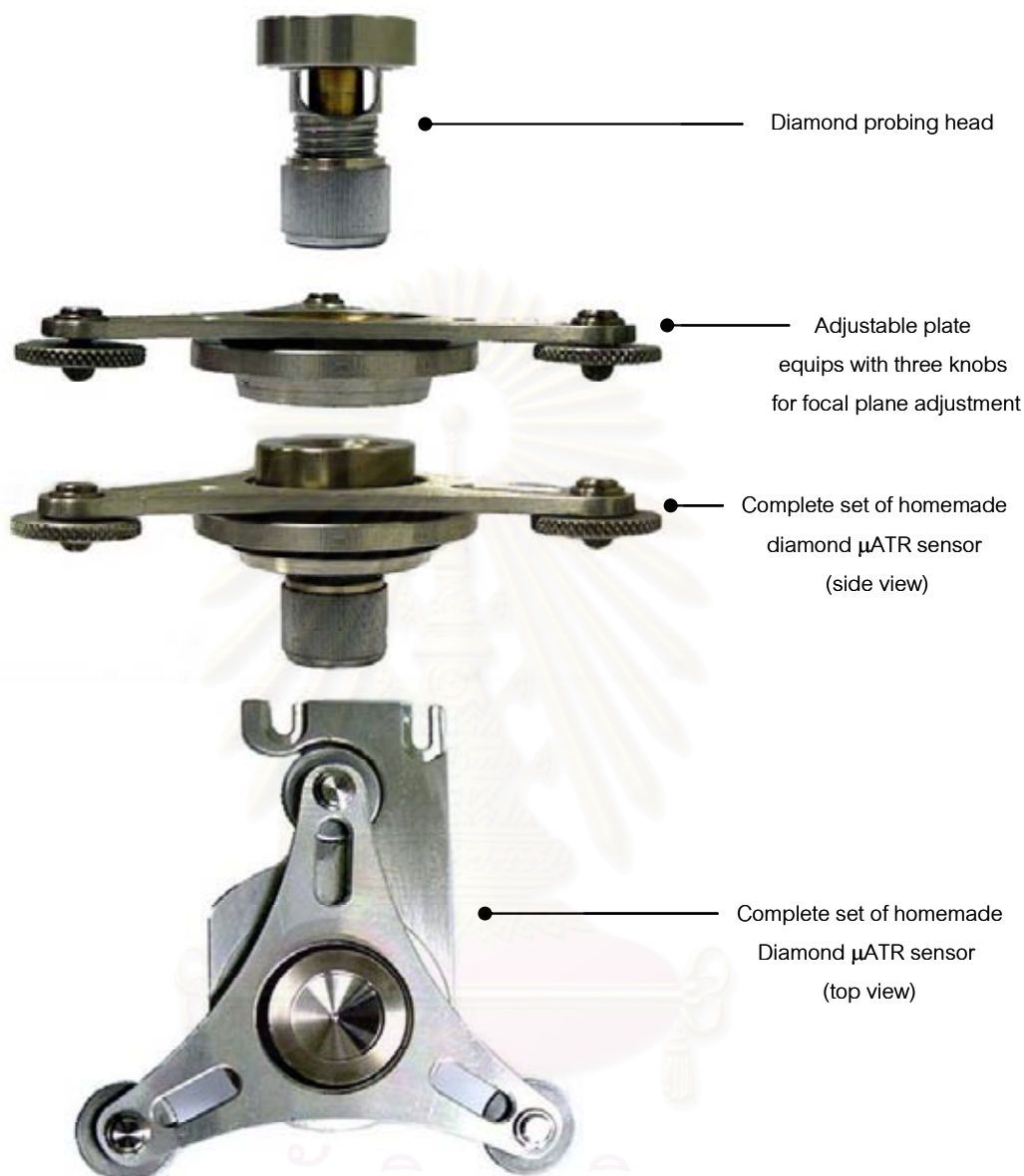


Figure 3.1 Composition of the homemade diamond μ ATR accessory: the diamond probing head, the adjustable reflection plane and complete set of homemade accessory.



Figure 3.2 The homemade diamond μ ATR accessory mounted onto the infrared microscope.

3.4 Surface Characterization by ATR FT-IR Spectroscopy

3.4.1 Experimental Procedure for the Conventional ATR Accessory

A commercial ATR accessory (the SeagullTM, Harrick Scientific, USA) with a hemispherical ZnSe IRE was employed for all conventional ATR spectral acquisition. The infrared radiation was coupled through the ZnSe IRE at the angle of incidence 45° . The single beam spectrum from the ZnSe IRE without sample was employed as a background for all ATR spectral acquisitions. For spectral acquisition of samples, liquid sample (mineral oil) was spread over ZnSe IRE as a liquid film while solid samples (*i.e.*, PVC, OPP/PE and Teflon/Polyimide/Teflon) was brought

into contact with the bottom surface of the IRE by applied pressure. The ATR spectra of samples were then acquired.

3.4.2 Experimental Procedure for Diamond μ ATR Sensor

For the novel diamond sensor experiment, all ATR spectra were performed on a NICPLANTM infrared microscope attached to the FT-IR spectrometer. A gem quality round brilliant cut natural diamond was employed as an IRE. For spectral acquisition of samples, liquid sample (mineral oil) was deposited as a liquid film on the culet of the diamond IRE while solid samples (*i.e.*, PVC, OPP/PE and Teflon/Polyimide/Teflon) were brought into contact with the culet of diamond IRE with an applied pressure. The table facet of diamond IRE was adjusted perpendicular to the incident radiation by using the adjusting knobs of homemade accessory to obtain the focal plane and maximum energy throughput. Its position was adjusted by x-y axis controlling stage of microscope. Reflection with normal incidence from the table facet of diamond IRE was employed as a background for all spectral acquisitions. The transmittance radiation was collected via the built-in 15X Cassegrainian objective through the table facet of diamond IRE. The ATR spectrum of the sample was acquired. The obtained spectrum was subtracted by transmittance spectrum of diamond, unique absorption band of the sample was revealed.

3.5 Depth Profiling by ATR FT-IR Spectroscopy

3.5.1 Experimental Procedure for the Conventional ATR Accessory

A commercial ATR accessory (the SeagullTM, Harrick Scientific, USA) was employed for ATR spectral acquisition. A hemispherical ZnSe was used as IRE and mounted into the ATR accessory. The angle of incidence was varied from 45° to 60° with a 5° interval. The background spectrum at an individual angle was collected. For spectral acquisition of samples, liquid sample (mineral oil) was placed as a liquid film onto the bottom surface of the IRE while solid samples (*i.e.*, PVC, OPP/PE and Teflon/Polyimide/Teflon) were brought into contact the bottom surface of the IRE

with an applied pressure. The ATR spectra at variable angles of incidence were acquired.

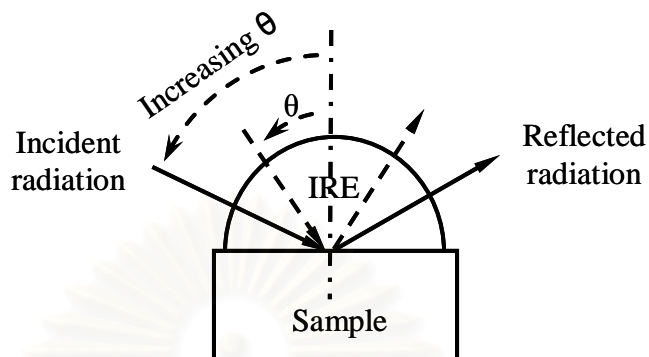


Figure 3.3 Schematic illustration of depth profiling using a hemispherical ZnSe IRE, variable angles of incidence.

3.5.2 Experimental Procedure for Diamond μ ATR Sensor

Constant Diamond Penetration with variable aperture

All ATR spectra were collected by a NICPLANTM infrared microscope attached to the FT-IR spectrometer. A gem quality round brilliant cut diamond IRE was mounted into the homemade accessory. For spectral acquisition of samples, liquid sample (mineral oil) was deposited as a liquid film on the culet of the diamond IRE while the solid samples (*i.e.*, PVC, OPP/PE and Teflon/Polyimide/Teflon) were brought into contact with the culet of diamond IRE by an applying highest pressure. The whole accessory was placed on the stage of the infrared microscope. The incident infrared radiation from the infrared microscope was coupled onto the table facet of the diamond IRE. The amount of infrared radiation is controlled by the aperture of the microscope. For the first spectra acquisition, the size of aperture was set to $100 \times 100 \mu\text{m}^2$. Reflection with normal incidence from the table facet of diamond IRE was employed as a background. Next step is raising the stage of microscope in order to bring the infrared radiation from infrared microscope via the 15x Cassegrainian objective. The infrared radiation was coupled into the pavilion facet of diamond through the table facet and the ATR radiation was collected. The spectrum of sample is then ratioed to the background. It is therefore important that

the aperture is the same for both background and sample spectra. The obtained spectrum was subtracted by transmittance spectrum of diamond, unique spectrum of the sample was revealed. The same procedure was repeated by increasing aperture size of the microscope (*i.e.*, 200x200, 300x300, 400x400 and 500x500 μm^2). The background and ATR spectra of sample at individual aperture were acquired before hand.

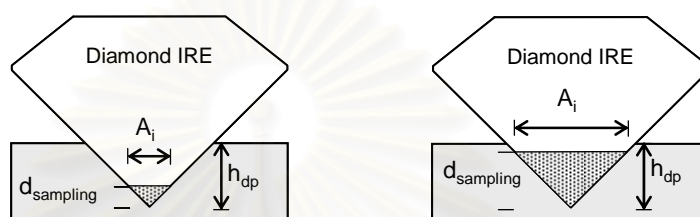


Figure 3.4 Schematic illustration of the depth-dependent measurement using a diamond IRE. The spectra were collected as varying aperture under a constant diamond penetration.

Varying Diamond Penetration under Constant Aperture

The NICPLANTM infrared microscope attached to the FT-IR spectrometer, was employed for all spectral acquisition. The diamond IRE was mounted into the homemade accessory. The solid samples (*i.e.*, PVC, OPP/PE and Teflon/Polyimide/Teflon) were placed against the culet of diamond IRE and then the pressure was applied. The homemade accessory was placed on the stage of the infrared microscope. The incident infrared radiation from the infrared microscope was coupled perpendicularly to the table facet of the diamond IRE. The amount of infrared radiation is controlled by the aperture of the microscope which was set at 200x200 μm^2 . Reflection with normal incidence from the table facet of diamond IRE was employed as a background for all spectral acquisition. The stage of microscope was raised in order to bring the infrared radiation from infrared microscope via the 15x Cassegrainian objective pass into the diamond IRE. The selected sampling area must focus at the culet of diamond IRE. The ATR FT-IR spectrum of sample was acquired. The obtained spectrum was subtracted by transmittance spectrum of diamond in order to acquire the characteristic absorption bands of the sample. The

same procedure was repeated by increasing applied pressure. By increasing the pressure, the diamond tip was penetrated deeper into the sample. Depth profiling by varying diamond penetration of diamond IRE under constant aperture were studied.

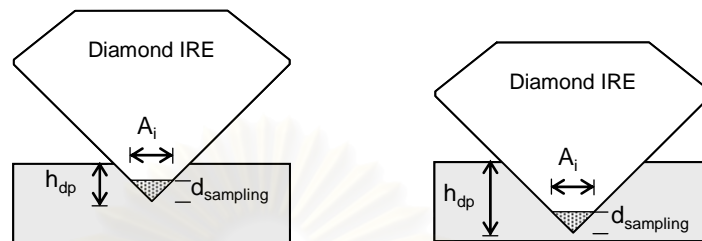


Figure 3.5 Schematic illustration of the depth-dependent measurement using a diamond IRE. The spectra were collected as the diamond penetrates deeper into the solid sample under a constant aperture.

CHAPTER IV

RESULTS AND DISCUSSION

4.1 Parameters Affecting Novel Diamond μ ATR Measurement

Before performing the surface characterization and/or depth profiling by the novel diamond μ ATR sensor, it is necessary to consider several parameters affecting the diamond μ ATR measurement. In order to verify the reproducibility and efficiency of the technique, the studies on diamond absorption, diamond arrangement, and variation of aperture were performed.

4.1.1 Characteristic Absorption of the Diamond IRE

Since diamond is absorbing in the mid-infrared region, absorptions at the characteristic frequencies of diamond are expected. Transflectance spectra of round brilliant cut diamonds with different magnitude of nitrogen and hydrogen impurities are shown in Figure 4.1. Diamond has three fundamental absorption bands in mid-infrared region, namely one-phonon absorption at 1400-900 cm^{-1} , two-phonon absorption at 2650-1500 cm^{-1} and three-phonon absorption at 3900-2650 cm^{-1} . The absorption magnitude in the one-phonon region depends strongly on the concentration of nitrogen impurity. Diamond with high nitrogen content always shows over absorption while that with low nitrogen content does show insignificant absorptions in this region. The two-phonon absorption is the intrinsic absorption of the diamond crystal structure. Although the two-phonon region is always over absorbing, it has little effect on the analysis of organic materials since most of the materials do not have absorption in this region. The three-phonon absorption is associated with hydrogen impurity. It imposes insignificant interference with the absorption of the materials since the absorption magnitude of diamond in this region is very weak.

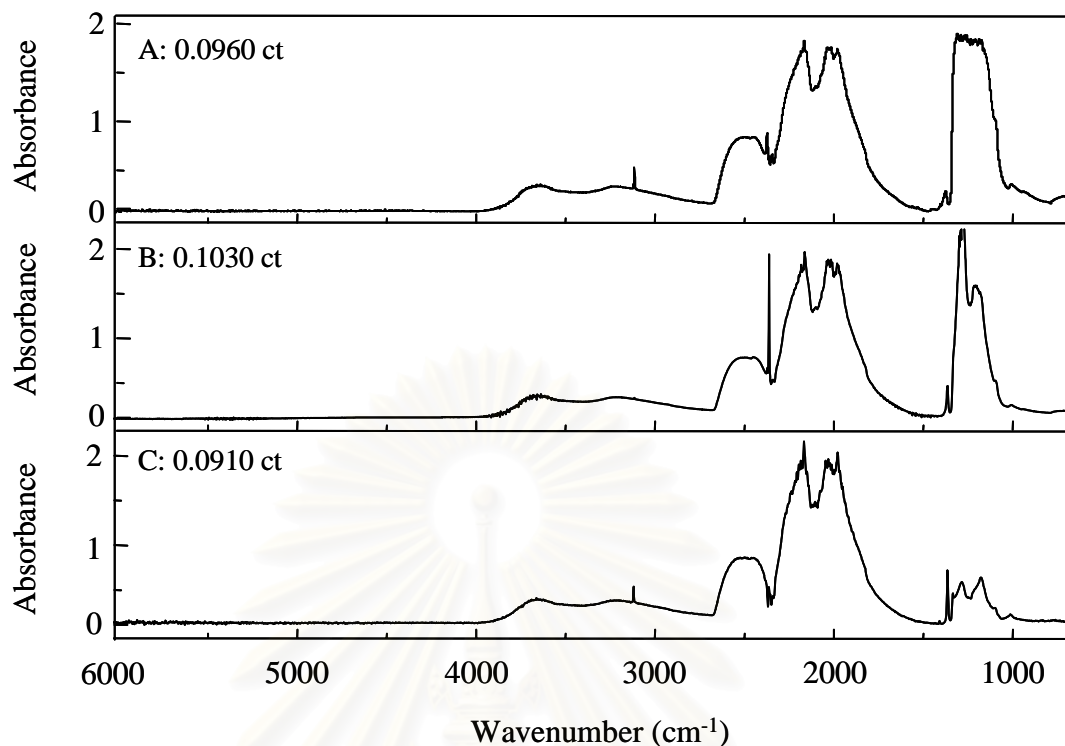


Figure 4.1 Transmittance spectra of round brilliant cut natural diamonds with different concentrations of nitrogen impurities.

A gem quality round brilliant cut diamond with a low nitrogen content was employed as an IRE for ATR measurements. The transmittance spectra of the diamond IRE is shown in Figure 4.2A. In the current spectral acquisition with the diamond μ ATR sensor, the specimen was simply brought into contact with the IRE and the ATR spectrum was acquired. The ATR spectrum of thick PVC attached to the culet of diamond IRE could be recognized as an additional absorption of the transmittance spectrum of the diamond IRE (Figure 4.2B). When the obtained spectrum was subtracted by the transmittance spectrum of diamond IRE, unique absorption bands of the sample was revealed (Figure 4.2C). By comparison, both the observed spectra of PVC by the diamond μ ATR sensor that obtained via the conventional ATR using 45° ZnSe IRE (Figure 4.2D) were the same. However, the ATR spectrum acquired by the diamond IRE was noticed the high noise level in the two-phonon region. This is due to the saturated absorption of the diamond. It is noted that the relative intensities in Figure 4.2C and D are different due to the nature of the incident radiation. The incident radiation in the conventional IRE is well-defined and

uniform (*i.e.*, 45°) while that in the novel diamond IRE consists rays with range of angles.

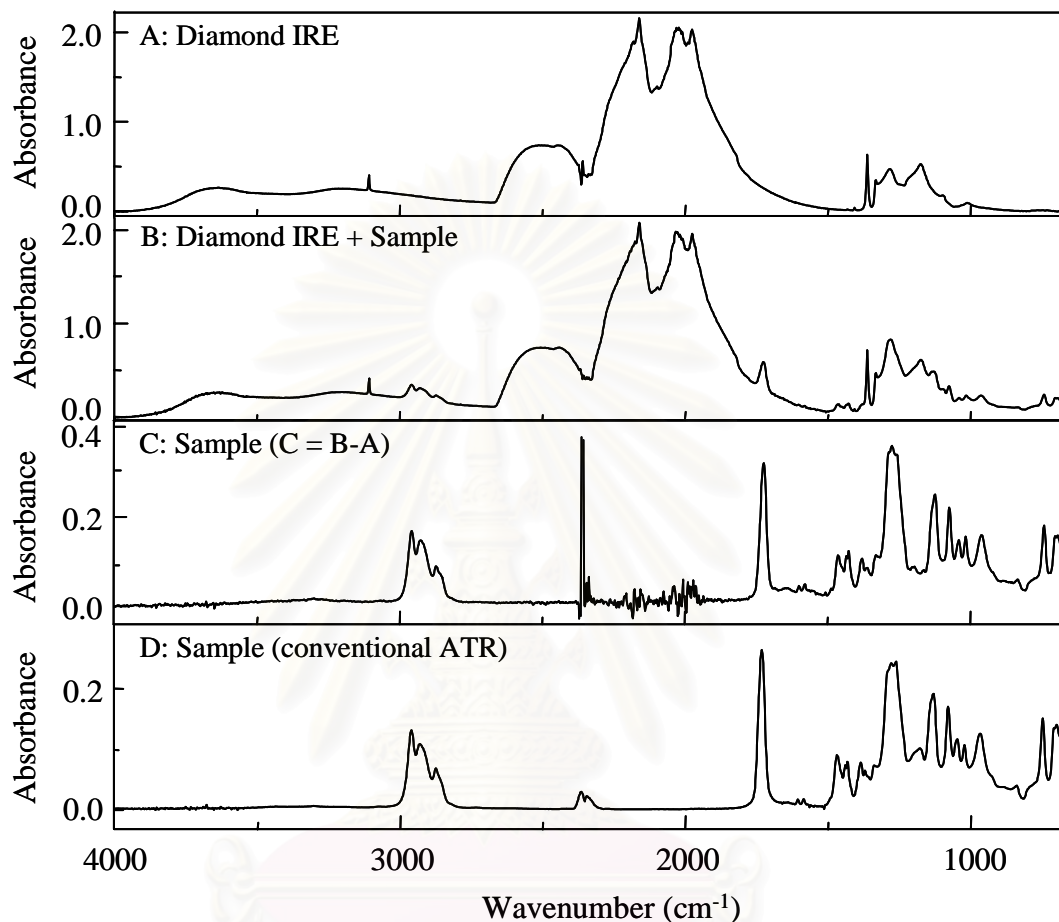


Figure 4.2 FT-IR spectra of PVC acquired by diamond μ ATR sensor: (A) spectrum of diamond IRE, (B) spectrum of PVC and diamond IRE, (C) spectrum of PVC when the contributions of diamond IRE was subtracted and (D) ATR spectrum of PVC obtained via conventional ZnSe IRE with 45° angle of incidence.

4.1.2 Diamond Arrangement

Transflectance spectra of the employed diamond IRE under different arrangements are illustrated in Figure 4.3. The diamond IRE was rotated by different angles with respect to a reference position. The superimposition of spectra shown in the inset is due to the homogeneous and isotropic nature of diamond. Although there

are some negligible discrepancies among the observed spectra due to minor variation associated with the diamond alignment, it does not have any influence on the observed ATR spectrum.

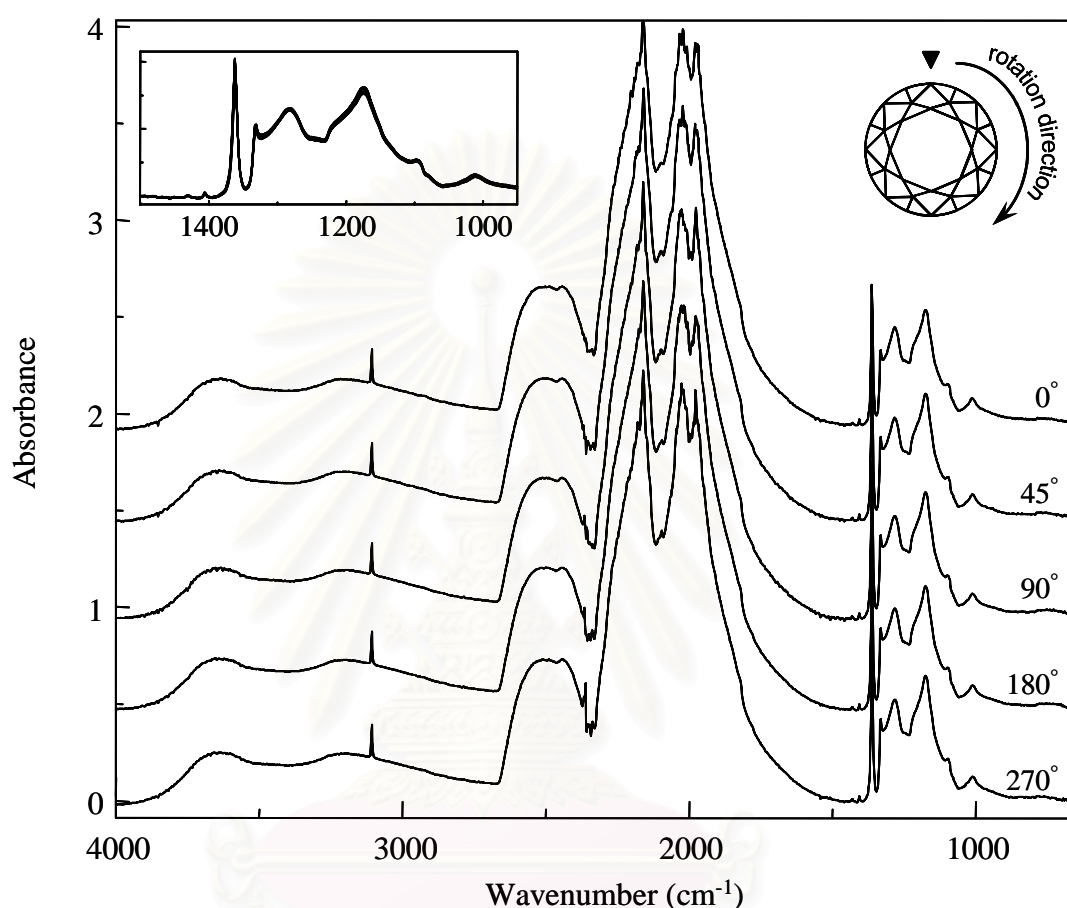


Figure 4.3 Transflectance spectra of a round brilliant cut diamond under different diamond orientations: 0°, 45°, 90°, 180° and 270° with respect to the reference position. The inset shows overlaid spectra in the one-phonon region.

To ensure the reproducibility of the novel diamond IRE, the liquid sample was spreaded as a liquid film onto the culet of the diamond. ATR spectra of the film were acquired different arrangement of diamond IRE. The mineral oil covers the culet and a portion of the pavilion facet near the culet. The normalized ATR spectra of a minute amount of mineral oil on the culet of the diamond IRE are shown in Figure 4.4. When the diamond IRE was rotated by different angles with respect to the reference position, the superimposition of the ATR spectra of the mineral oil in the

C-H stretching mode was shown in the inset of Figure 4.4. As a result, the acquired spectra were not affected by the arrangement of the diamond IRE.

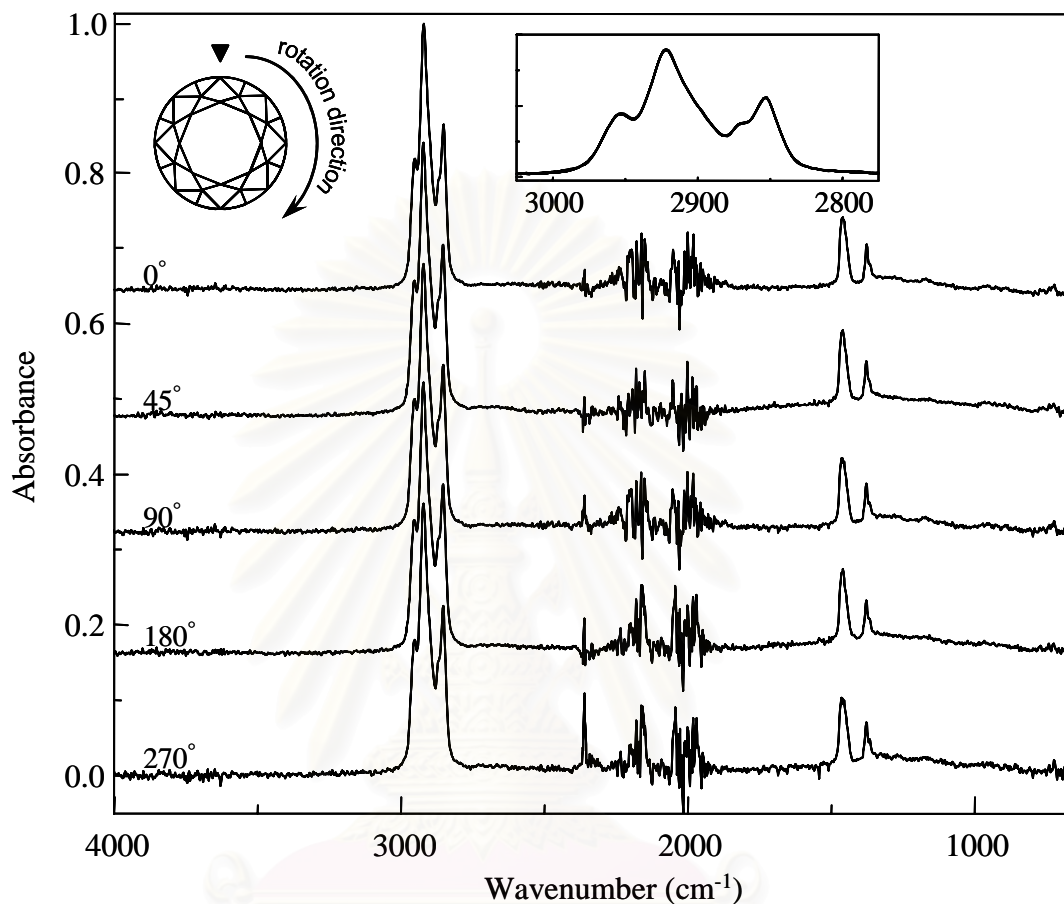


Figure 4.4 Normalized ATR spectra of a mineral oil on the diamond IRE under different diamond rotation. The diamond was rotated at 0°, 45°, 90°, 180° and 270° with respect to the reference position. The inset shows the superimposition of the ATR spectra of the mineral oil in the C-H stretching region.

4.1.3 Variation of Apertures

In case of infrared microscope, the amount of infrared radiation that impinges on the diamond IRE (or sample) can be controlled by the aperture of the microscope. The variable aperture is useful to study the different areas of the sample and depth dependent analysis. Prior to characterization of the depth profiling, the performance of infrared microscope with varying aperture sizes was investigated.

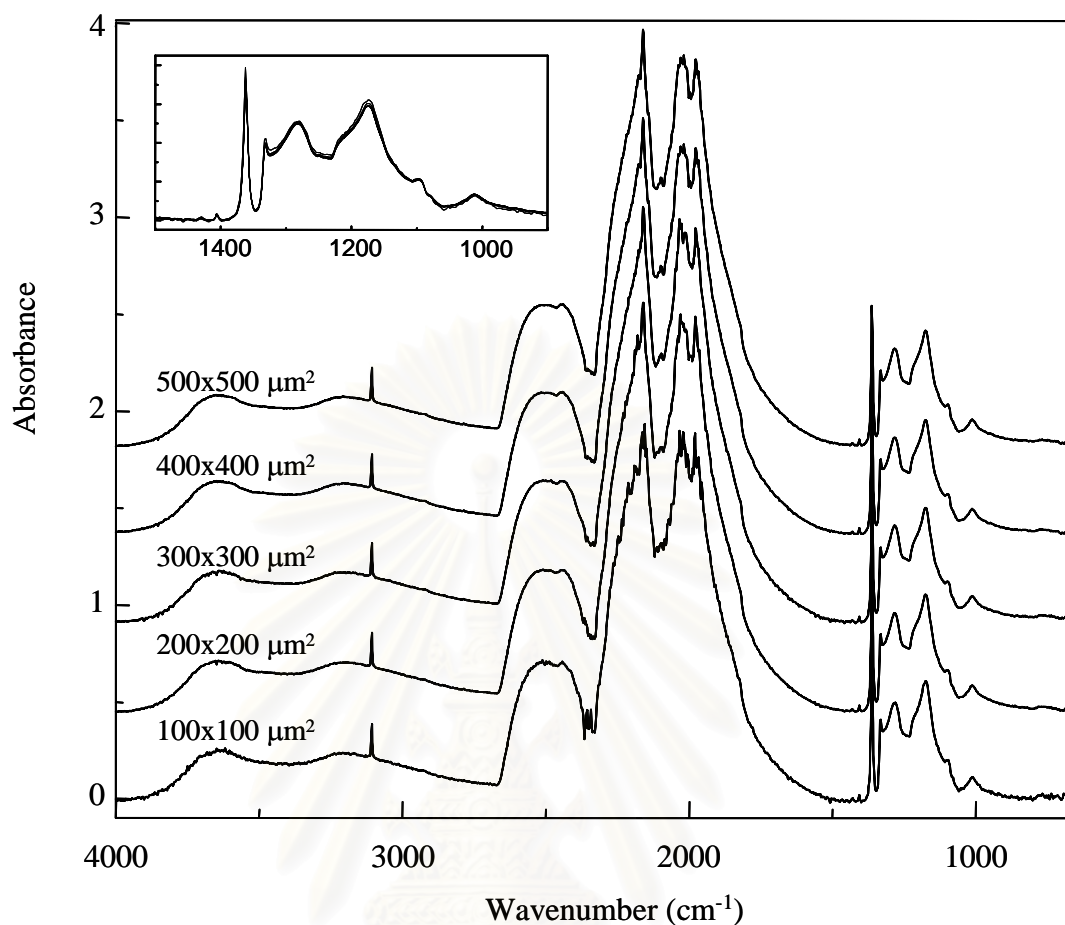


Figure 4.5 Normalized transmittance spectra of a round brilliant cut diamond under varying the aperture sizes of infrared microscope.

The normalized transmittance spectra of diamond IRE under different aperture size setting are shown in Figure 4.5. All obtained transmittance spectra illustrate the same spectral feature of diamond IRE. The obtained spectra show the prominent characteristic absorption of the diamond IRE with different signal-to-noise ratio. When the larger size of aperture was employed, the observed spectra show the better signal-to-noise ratio and spectral quality. In case of the small aperture, the lower energy throughput results in high noise level of acquired spectrum. However all obtained spectra obviously reveal the same spectral intensity, it indicates that the variation of aperture do not affect the ATR operation.

4.2 Surface Characterization of Homogeneous Samples

ATR FT-IR spectroscopy is a powerful surface characterization. The major problem in ATR technique is the contact between IRE and sample. In order to get a good-quality ATR spectrum, an optical contact between IRE and sample must be achieved. To confirm the qualitative spectral acquisition using the diamond μ ATR sensor, the material being investigated must have a good optical contact with the IRE such as liquid and soft solid samples. The applicability of surface characterization by novel diamond IRE is compared with those of the conventional ZnSe IRE.

4.2.1 Mineral Oil

The ATR spectra of mineral oil acquired by the novel diamond μ ATR sensor and conventional ATR technique are shown in Figure 4.6. The obtained spectra clearly reveal characteristic absorption bands of the mineral oil. Since the sample was deposited as a liquid film onto the IRE, a good contact between the sample and the surface of the IRE were obtained. By comparison, the spectrum obtained from the diamond μ ATR sensor is the same as that from the conventional ATR technique using 45° ZnSe IRE.

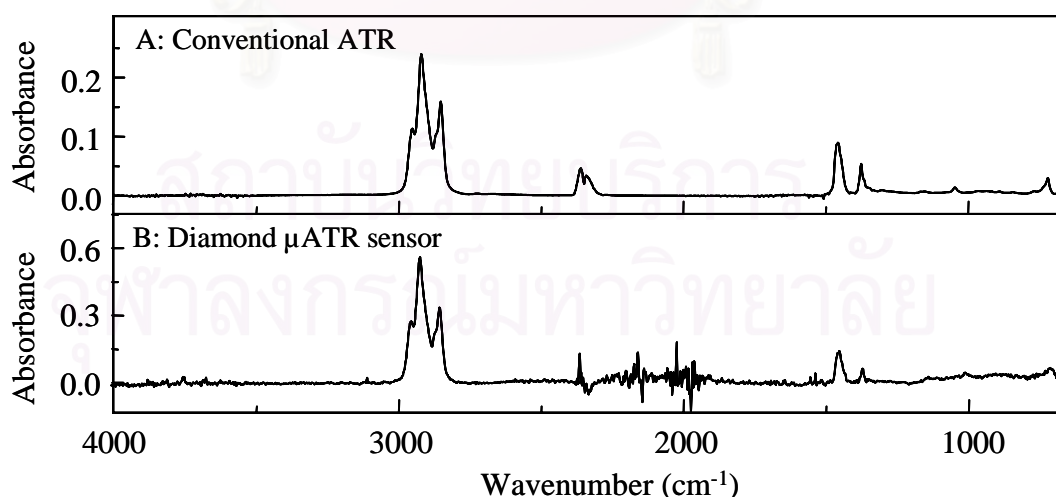


Figure 4.6 ATR spectra of mineral oil acquired by two sampling techniques: (A) conventional ATR using 45° ZnSe IRE and (B) diamond μ ATR sensor.

4.2.2 Poly(vinyl chloride)

The ATR spectra of thick PVC acquired by conventional ATR and diamond μ ATR sensor are shown in Figure 4.7. Since PVC is a soft and flexible solid, a good contact between its surface and the IREs can be achieved. The obtained ATR spectra acquired from both techniques show the same features. This implies that the novel diamond μ ATR sensor can be employed for surface characterization.

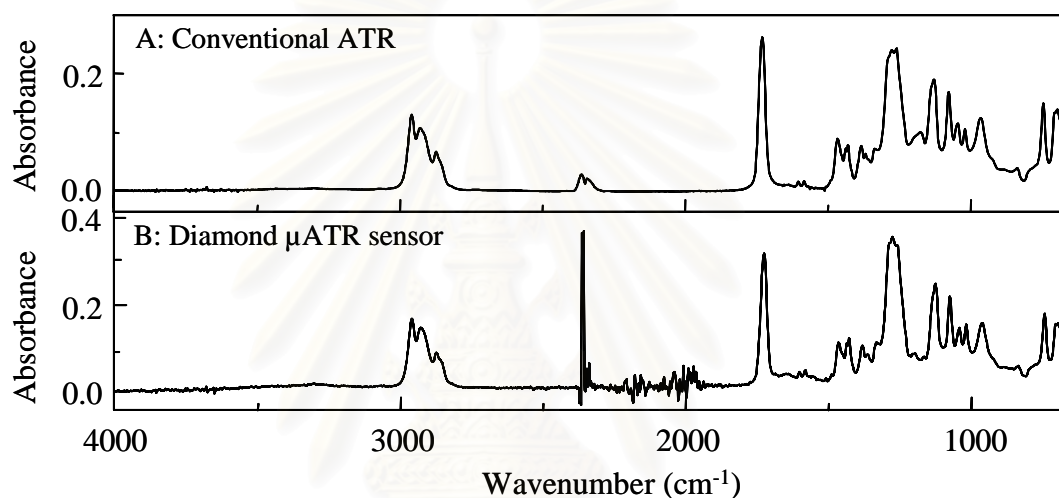


Figure 4.7 ATR spectra of PVC acquired by two sampling techniques: (A) conventional ATR using 45° ZnSe IRE and (B) diamond μ ATR sensor.

4.3 Depth Profiling of Homogeneous samples

In order to demonstrate the efficiency of the novel diamond μ ATR sensor for depth profiling analysis, the homogeneous sample that can be achieved a good contact with IRE was first studied. For the ATR experiments, the depth dependent measurement can be divided into two methods: (1) conventional ATR technique using ZnSe IRE and (2) diamond μ ATR sensor. The observed ATR spectra acquired with the novel diamond IRE will be compared to those acquired with a traditional ZnSe IRE.

4.3.1 Mineral Oil

4.3.1.1 Conventional ATR technique

Depth profiling by conventional ATR technique was performed by varying the angle of incidence of the SeagullTM accessory. The normalized ATR spectra of mineral oil acquired by conventional ZnSe IRE with the angle of incidences of 45°, 50°, 55° and 60° are shown in Figure 4.8. It should be noted that changing of the angle of incidence affects on the penetration depth. If the angle of incidence is decreased, the penetration depth increased. The greater penetration depth implies a greater distance from surface of the sample where chemical information can be observed by the obtained ATR spectrum. Since the mineral oil is a homogeneous liquid sample, all observed spectra in the inset of Figure 4.8 show the same characteristic absorption bands of mineral oil.

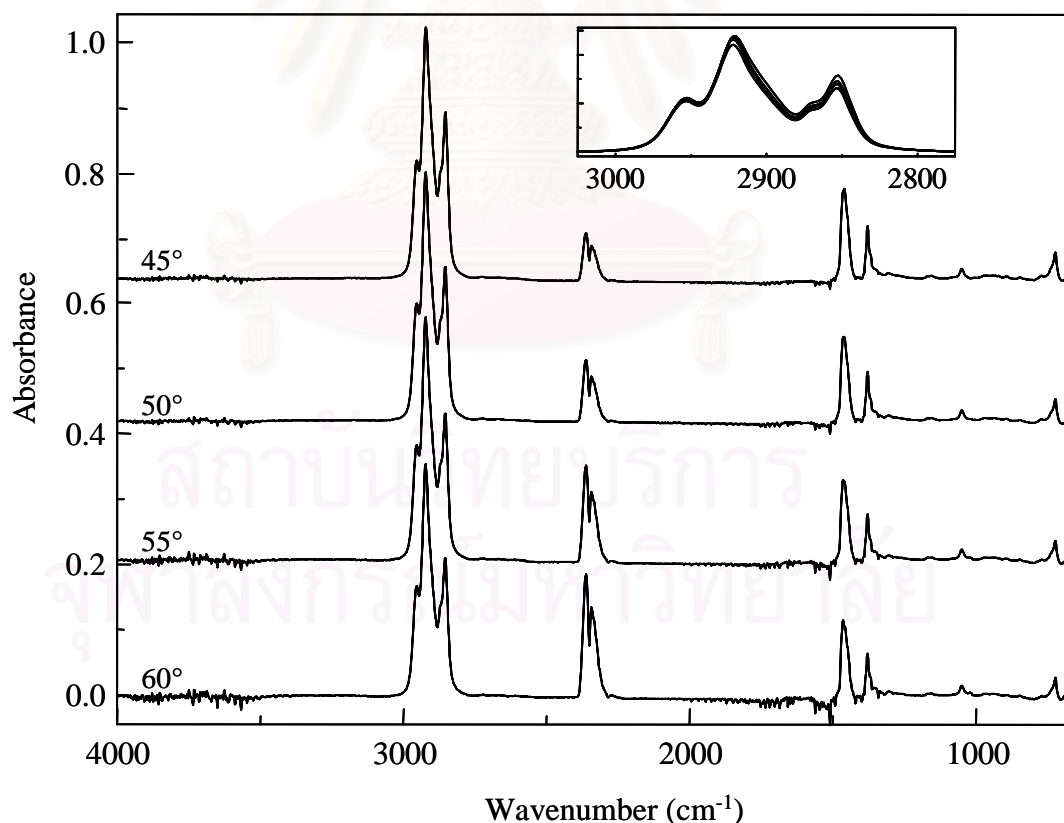


Figure 4.8 Normalized ATR spectra of mineral oil acquired by conventional ATR using ZnSe IRE. The angle of incidence was varied from 45° to 60° with a 5° interval.

4.3.1.2 Diamond μ ATR technique

To investigate the depth profiling capability of the novel diamond IRE, a liquid sample was analyzed. ATR spectra of a minute amount of mineral oil deposited on the culet of diamond IRE while the aperture of infrared microscope were set at 100×100 , 200×200 , 300×300 , 400×400 and $500 \times 500 \mu\text{m}^2$ are shown in Figure 4.9B. In principle, changing the aperture size affects the illuminated area and the thickness of sample. The spectral feature of sample with greater thickness can be acquired by increasing the size of aperture. However, the observed spectra show the chemical information of mineral oil with the same absorption magnitude since mineral oil is a homogeneous liquid sample.

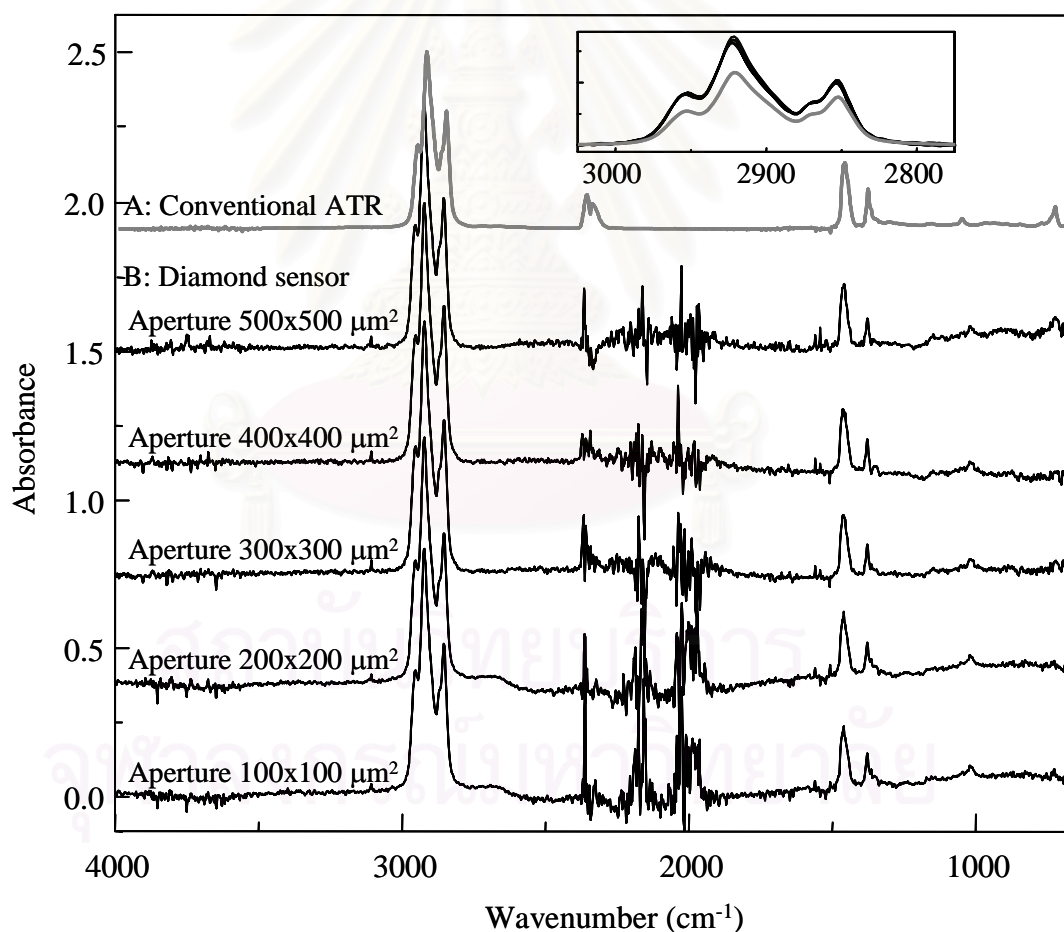


Figure 4.9 Normalized ATR spectra of mineral oil: (A) spectrum acquired by conventional ATR (B) depth profiling by the diamond μ ATR sensor, the aperture of microscope were set at 500×500 , 400×400 , 300×300 , 200×200 and $100 \times 100 \mu\text{m}^2$.

4.3.2 Poly(vinyl chloride)

4.3.2.1 Conventional ATR technique

In order to verify the depth profiling study of solid sample, the variable incident angle by conventional ATR technique was employed. The normalized ATR spectra of PVC with varying the angle of incidence from 45° to 60° with a 5° interval are shown in Figure 4.10. Since the PVC is a homogeneous solid, spectra with the same spectral feature were observed as the angle of incidence increased.

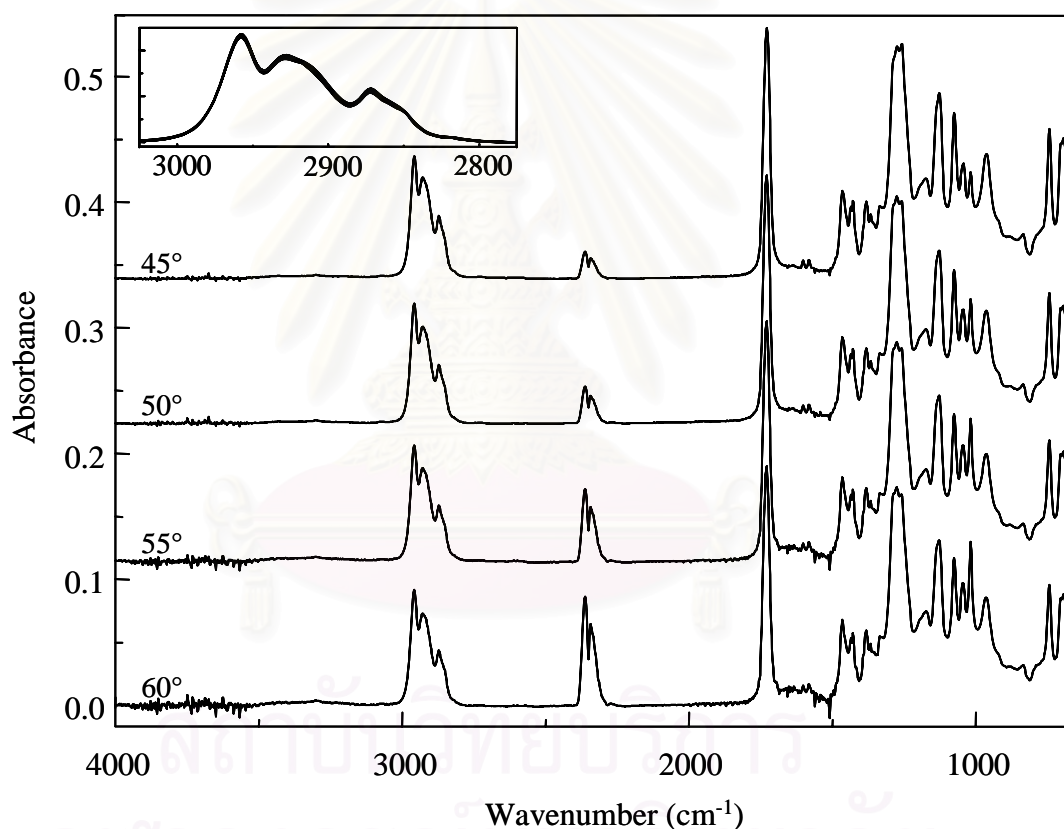


Figure 4.10 Normalized ATR spectra of PVC acquired by conventional ATR using ZnSe IRE. The angle of incidence was varied from 45° to 60° with a 5° interval.

4.3.2.2 Diamond μ ATR technique

In order to demonstrate the efficiency of the novel diamond μ ATR sensor for depth profiling analysis of solid sample, the depth profiling measurement can be divided into two procedures: (1) varying diamond penetration under constant aperture size and (2) constant diamond penetration with varying aperture size.

Varying diamond penetration under constant aperture

For depth profiling analysis by the diamond μ ATR sensor, the solid sample was brought into contact with the culet of the diamond IRE by applied pressure. The diamond tip (*i.e.*, the culet and a portion of pavilion facet of diamond IRE) was penetrated into the sample as the pressure was increased. The normalized ATR spectra of PVC by increasing the diamond penetration under constant aperture are shown in Figure 4.11B. The spectral information at a greater depth can be acquired by pressing the diamond tip deeper into the sample. Since PVC is a homogeneous solid, all observed spectra show the same spectral feature. The inset of Figure 4.11 shows superimposition of the absorption bands in C-H stretching region. This result suggested that the diamond μ ATR sensor can be applied for depth dependent analysis without an influence of environmental and/or experimental conditions.

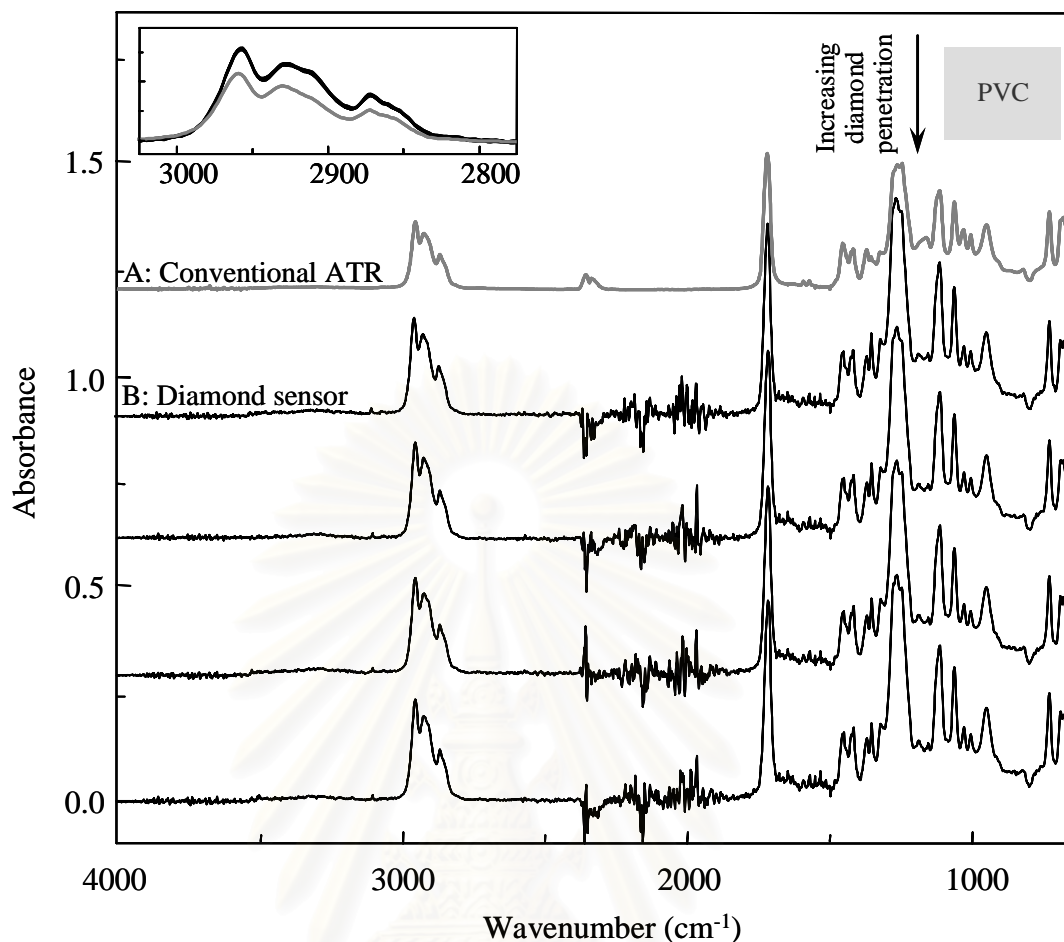


Figure 4.11 Normalized ATR spectra of PVC: (A) spectrum acquired by conventional ATR (B) depth profiling by increasing diamond penetration under a constant aperture of the diamond μ ATR sensor.

Constant diamond penetration with varying aperture

Depth profiling of a solid sample was also performed by the diamond μ ATR sensor which the constant diamond penetration with varying the size of aperture, as illustrated in Figure 4.12B. The PVC was pressed against the diamond IRE with a maximum penetration while the aperture was set at 500x500, 400x400, 300x300, 200x200 and 100x100 μm^2 . Due to the varied aperture operation affects depth dependent information by changing the thickness of sampling layer and the illuminating area. If a small aperture was employed, the spectral information of a thin layer at the culet will be acquired. If a larger aperture was employed, the spectral information of a thicker film will be acquired. Due to the homogeneity of PVC

sample, all observed spectra show the same spectral feature. However there are the same negligible discrepancies among the observed spectra due to noise level associated with the size of the aperture. In case of a larger aperture, the acquired spectrum shows better signal-to-noise ratio and spectral quality. The obtained spectrum with the small aperture is presenting the high noise level. However, the ATR spectra obtained from different aperture sizes clearly reveal the same absorption magnitude as shown in the inset of Figure 4.11.

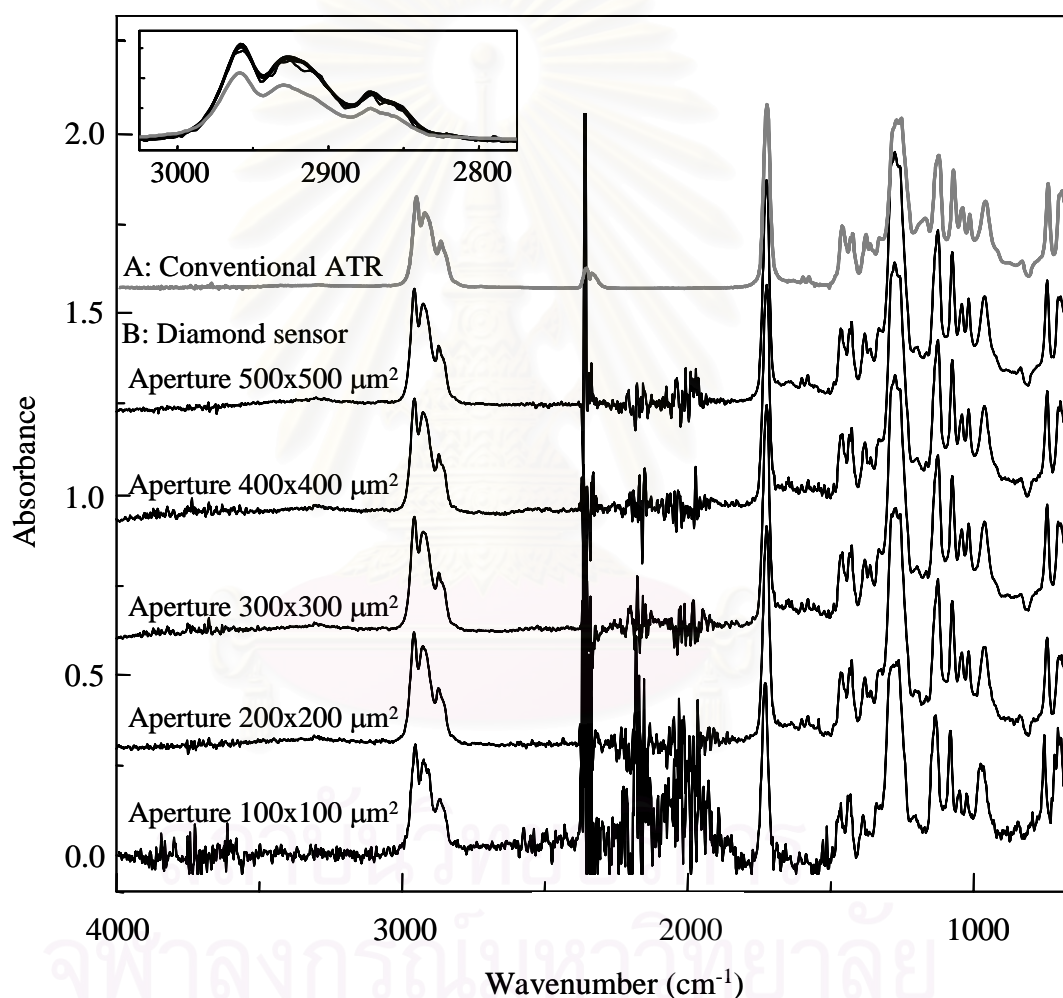


Figure 4.12 Normalized ATR spectra of PVC: (A) spectrum acquired by conventional ATR and (B) depth profiling by variable the aperture under a constant diamond penetration of the diamond μ ATR sensor.

4.4 Surface Characterization of Heterogeneous Samples

4.4.1 OPP/PE

To demonstrate the surface characterization capability of the diamond IRE, a bi-layered film of a 15 μm oriented polypropylene (OPP) film coated on a 20 μm polyethylene (PE) film was analyzed. ATR spectra of both sides of the bi-layered film acquired by the novel diamond IRE and conventional ZnSe IRE are shown in Figure 4.13. The obtained spectra clearly reveal characteristic absorption frequencies of the OPP and PE. Comparison between diamond μATR technique and conventional ATR technique, it indicates that the spectral acquisition by the diamond μATR sensor is the same as that obtained by conventional ATR technique.

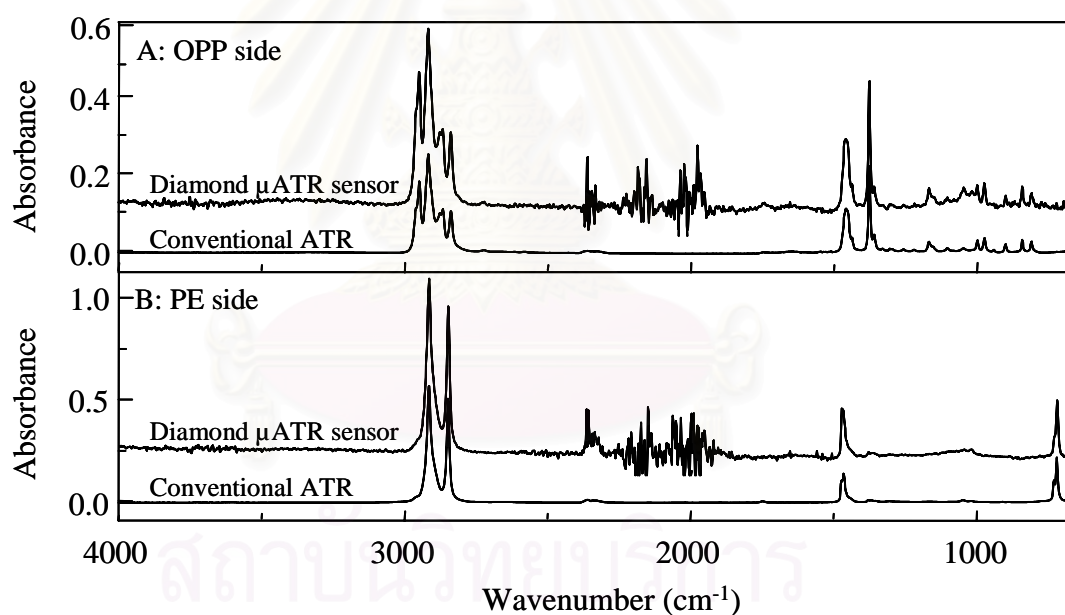


Figure 4.13 ATR spectra of both side of OPP/PE bi-layered film: (A) OPP side and (B) PE side. The spectra were acquired by conventional ATR using 45° ZnSe IRE and the diamond μATR sensor.

4.4.2 Teflon/Polyimide/Teflon

For surface characterization of multilayered film, it is necessary to recognize the individual layers and analyze each of the constituent part of the sample. The Teflon/Polyimide/Teflon multilayered film was separated to each of layers, and then the individual layer was placed against the IRE for spectral acquisition. ATR spectra of individual layers of Teflon/Polyimide/Teflon acquired by the traditional ZnSe IRE and the novel diamond IRE are shown in Figure 4.14. The obtained spectra of both techniques indicate the chemical information of Teflon (outside), Polyimide and Teflon (inside), respectively.

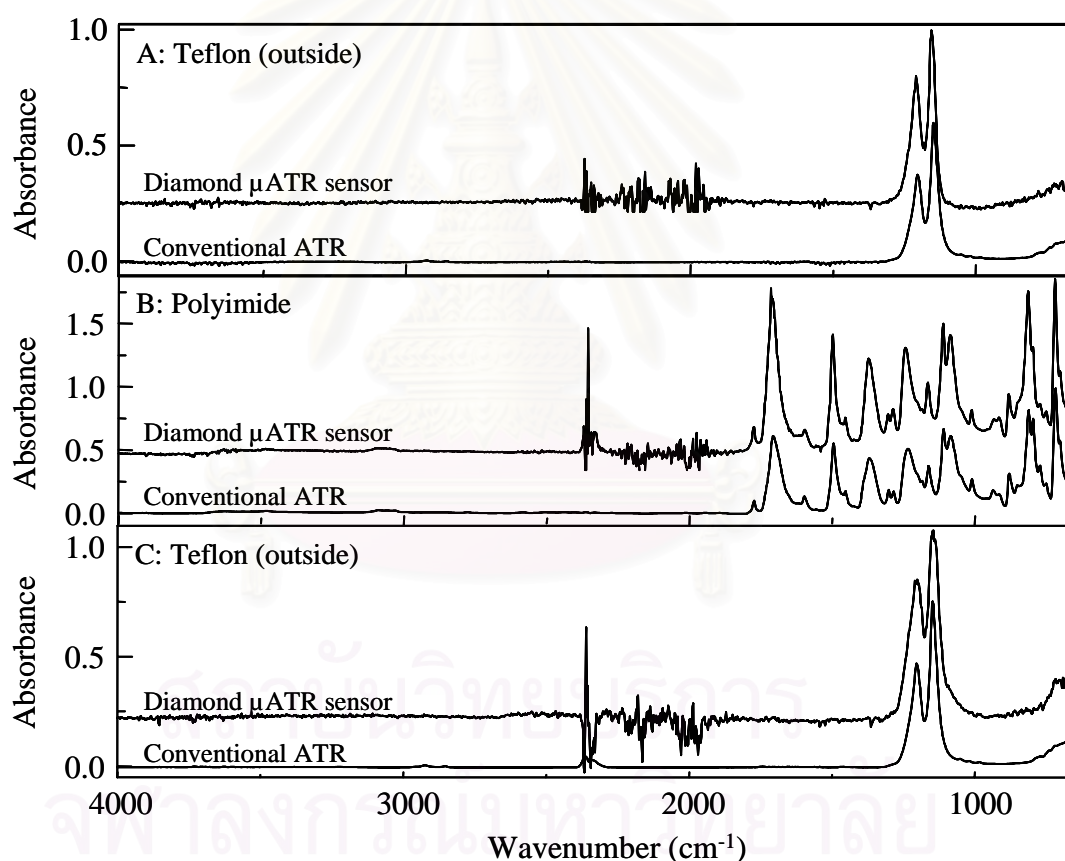


Figure 4.14 ATR spectra of individual layers of Teflon/Polyimide/Teflon multilayered film acquired by two sampling techniques: conventional ATR using 45° ZnSe IRE and the diamond μ ATR sensor.

4.5 Depth Profiling of Heterogeneous Samples

4.5.1 OPP/PE

4.5.1.1 Conventional ATR

Depth profiling analysis was performed by conventional ATR technique in which the sample and IRE are in intimate contact. For ATR experiment, total internal reflection occurs and an evanescent field penetrates in the sample. A set of angle dependent spectra can be employed for depth profiling of a non-homogeneous material.

In order to demonstrate the depth profiling analysis of the conventional ATR technique, a bi-layered film of the oriented polypropylene (OPP, 15 μm) coated on polyethylene (PE, 20 μm) was analyzed. The OPP side was placed against the surface of ZnSe IRE, the angle of incidence was set at 45°, 50°, 55° and 60°. The spectral features of the bi-layered film as that shown in Figure 4.15 were observed. All normalized ATR spectra show only chemical absorption bands of OPP. The spectra indicate that no spectral change was detected. Due to the decay of the evanescent field, only shallow depth dependent information up to few micrometers from the surface can be obtained from ATR spectra. As a result, the chemical information beyond the distance where the field amplitude decays to an insignificant level cannot be acquired by conventional ATR measurement.

สถาบันวิทยบริการ
จุฬาลงกรณ์มหาวิทยาลัย

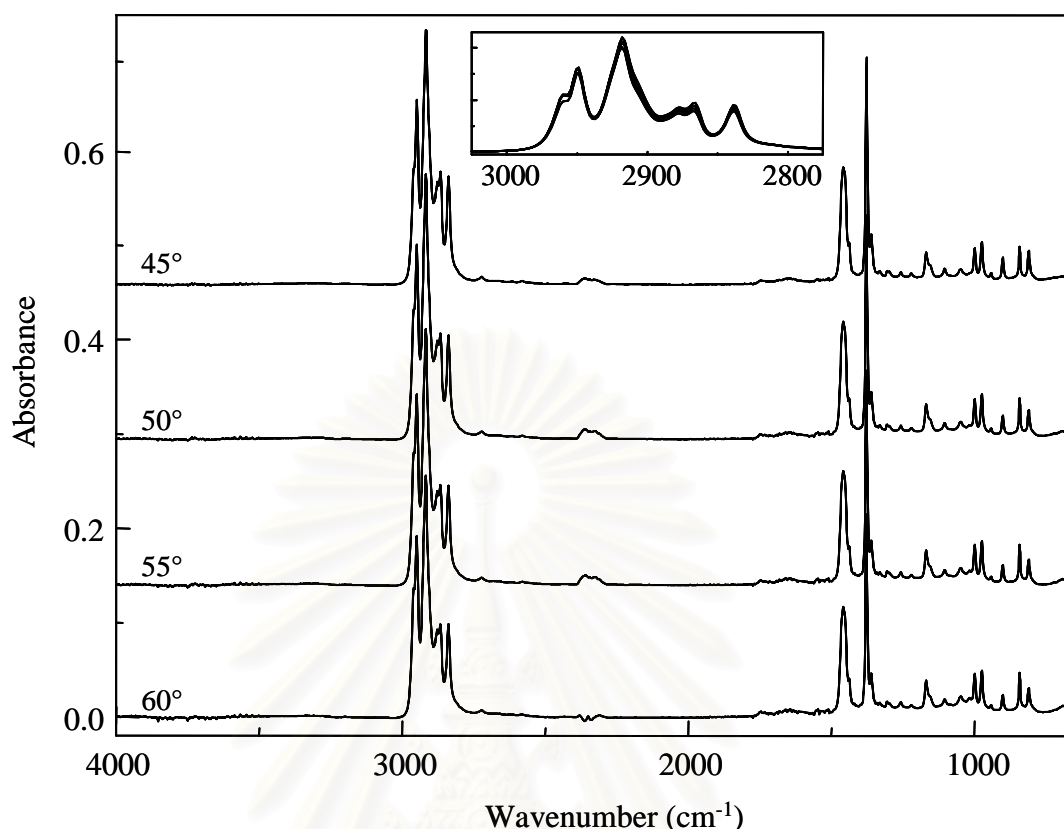


Figure 4.15 Normalized ATR spectra of OPP/PE bi-layered film acquired by conventional ATR using ZnSe IRE. The angle of incidence was varied from 45° to 60° with a 5° interval.

4.5.1.2 Diamond μ ATR sensor

The novel diamond μ ATR sensor can perform depth profiling of heterogeneous sample. Since diamond is the hardest known material, it can penetrate into the hard and rigid solid specimen simply by pressing the sample against the diamond IRE. By performing controlled penetration of the diamond IRE through the sample and/or illuminating the pavilion facet near the culet with various aperture sizes, spectral information of a specific layer at a certain distance from the surface can be selectively collected. The illuminated portion of the diamond tip near the culet can be adjusted via the opening aperture of the focusing optics. Thus, only parts of the material attached to the diamond IRE at the illuminated pavilion facet interacted with the coupled radiation and have contribution in the observed spectrum. Based on the brilliant-cut shape and the experimental operation with an infrared microscope,

two modes of depth profiling techniques can be performed by the diamond IRE: variable diamond penetration under constant illuminating aperture and varying aperture under constant diamond penetration operations.

Varying diamond penetration under constant aperture

Depth profiling of bi-layered film (OPP/PE) using the novel diamond IRE was performed by varying the diamond penetration with fixed the size of aperture. Diamond IRE can penetrate into the specimen by pressing the specimen against the diamond IRE, since diamond is the hardest known material. The chemical information of OPP/PE bi-layered film were observed as an increasing pressure was applied in order to increase the diamond penetration from the OPP side as shown in Figure 4.16B. The inset of Figure 4.16 shows the characteristic absorption bands in C-H stretching region ($3025\text{-}2775\text{ cm}^{-1}$). At lowest applied pressure, the characteristic absorption bands of OPP appeared at 2952 , 2915 , 2866 and 2833 cm^{-1} which confirmed by the same chemical information at the surface of OPP/PE using conventional ATR technique (Figure 4.16A). When the diamond penetration increased, the intensity of OPP bands in C-H stretching region at 2952 , 2915 , 2866 and 2833 cm^{-1} decrease while the intensity at 2910 and 2845 cm^{-1} bands continue to increase. The appearances of new bands at 2910 and 2845 cm^{-1} reveal the chemical information of PE that confirmed by surface characterization of PE/OPP film using conventional ATR technique (Figure 4.16C). The observed spectra indicate that the novel diamond μ ATR sensor in this operation can detect the change of spectral feature from that of the OPP to that the PE as the diamond tip penetrated deeper into the OPP/PE bi-layered film.

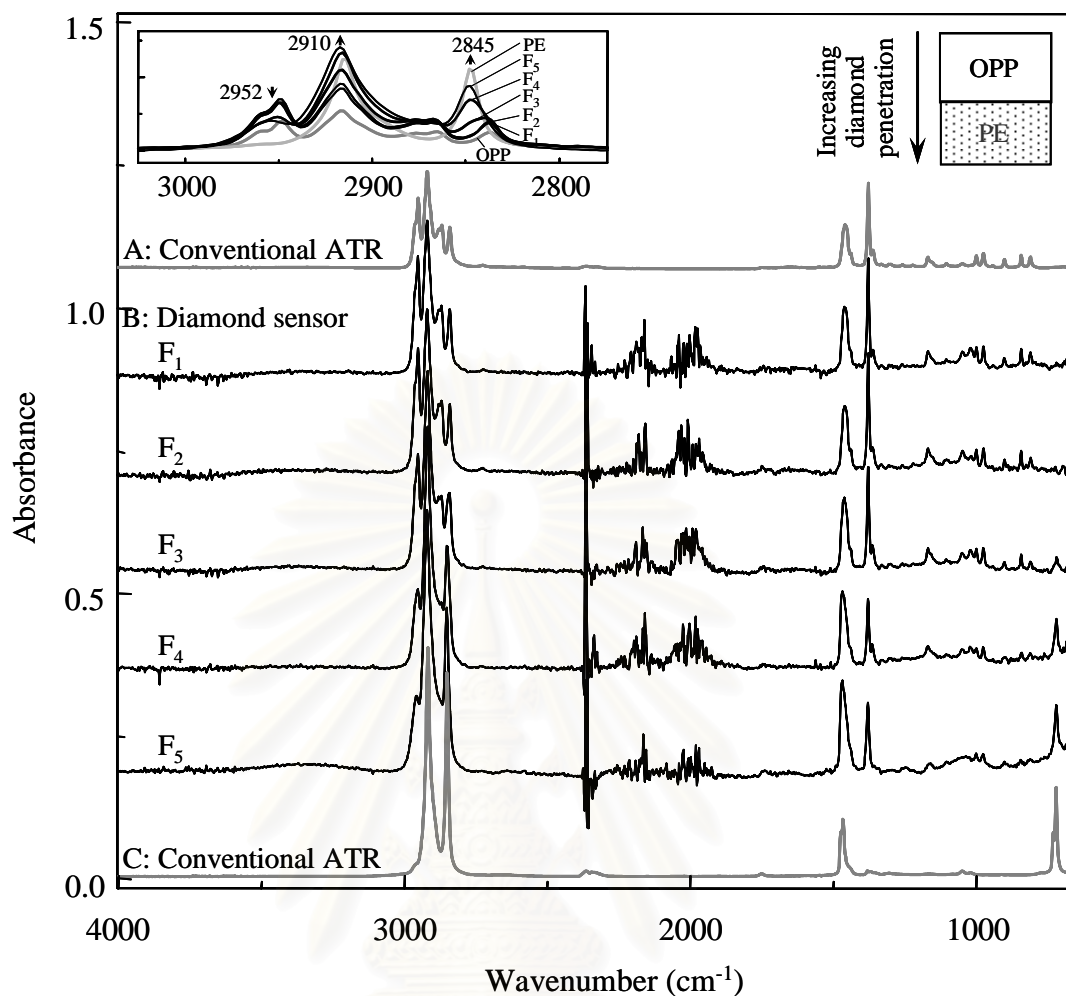


Figure 4.16 Normalized ATR spectra of OPP/PE: (A) spectra of OPP acquired by conventional ATR, (B) depth profiling of OPP/PE by increasing diamond penetration under a constant aperture of the diamond μ ATR sensor, F_i denote the applied force that $F_1 < F_2 < F_3 < F_4 < F_5$ and (C) spectrum of PE acquired by conventional ATR.

Constant diamond penetration with varying aperture

The ATR spectra recorded from the same specimen using the diamond μ ATR sensor with varying the aperture size under a constant diamond penetration are shown in Figure 4.17B. The diamond was penetrated into the OPP/PE bi-layered film from the OPP side while the aperture was set at 500×500 , 400×400 , 300×300 , 200×200 and $100 \times 100 \mu\text{m}^2$. Since the aperture of infrared microscope is controlling the amount of infrared radiation that impinges on the sample, the varying aperture is

useful to analyze the different area of the heterogeneous sample. When a small aperture was employed, the observed spectrum was dominated by the chemical absorption bands in C-H stretching mode at 2910 and 2845 cm^{-1} . This indicated that the diamond tip was penetrated deeper into the film and position at the PE layer. When the larger apertures were employed, the absorption magnitude in C-H stretching mode of PE at 2910 and 2845 cm^{-1} decrease while the magnitude of OPP in C-H stretching mode at 2952, 2915, 2866 and 2833 cm^{-1} increase according to the thicker of sampling depth. At the largest aperture, the spectral feature shows the prominent band of OPP. This observation indicates that the novel diamond μ ATR sensor in this condition can be detected the change of chemical species of OPP/PE film as the varying aperture sizes of couple radiation.

A direct comparison between the conventional ATR and diamond μ ATR spectra measured under the same specimen show spectral differences. The ATR spectra acquired by conventional ATR present the spectral information associated with the chemical species of the OPP film (Figure 4.15) while those acquired by the diamond μ ATR sensor show the surface and bulk chemical information exhibiting different chemical species of bi-layered film as shown in Figure 4.16B and 4.17B. The observed phenomena suggested that the novel diamond μ ATR sensor can be employed for depth profiling purpose where the chemical information below the surface of solid sample can be selectively acquired.

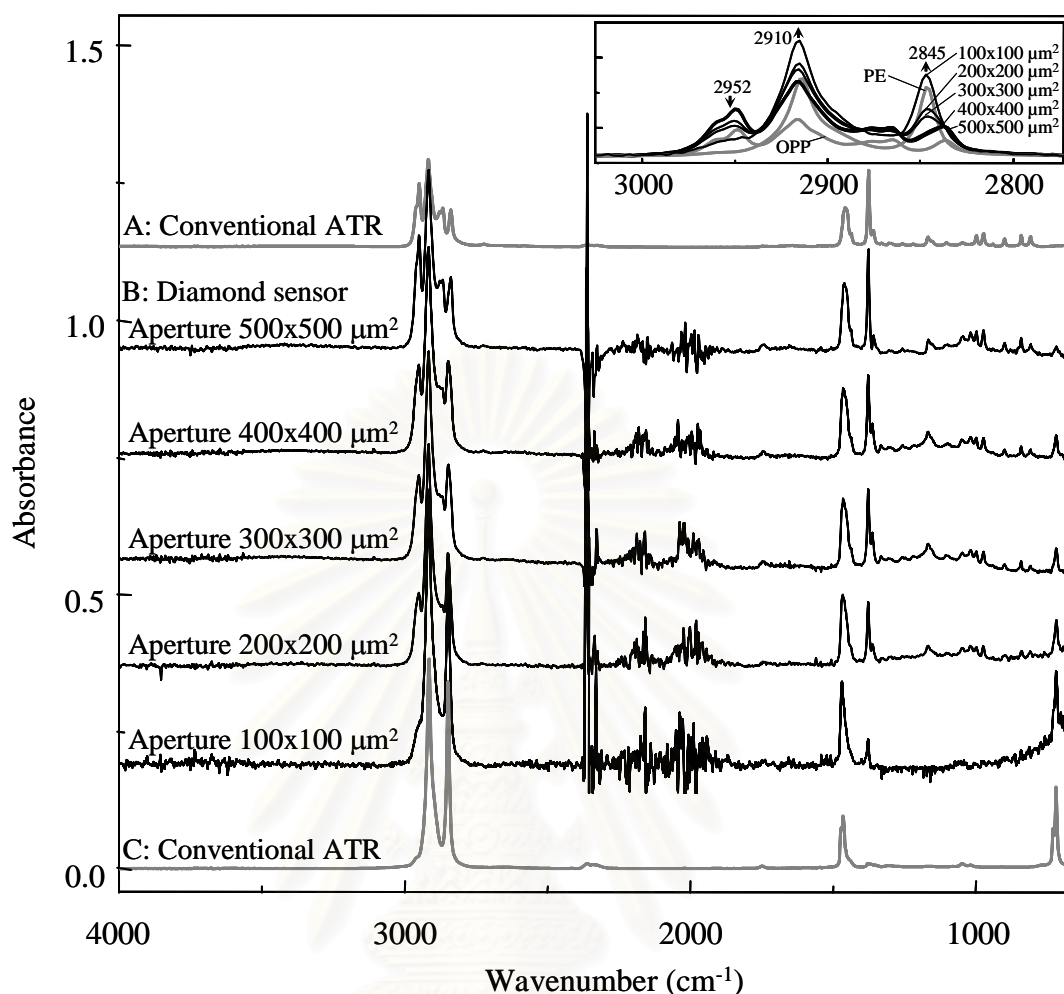


Figure 4.17 Normalized ATR spectra of OPP/PE: (A) spectrum of OPP acquired by conventional ATR, (B) depth profiling of OPP/PE by increasing aperture under a constant diamond penetration of the diamond μ ATR sensor and (C) spectrum of PE by conventional ATR.

4.5.2 Teflon/Polyimide/Teflon

4.5.2.1 Conventional ATR

In order to verify the depth dependent analysis of multilayered film, the varying incident angle by conventional ATR technique was employed. A multilayered film of Teflon (12.4 μm)/polyimide (25.4 μm)/Teflon (12.4 μm) was placed against the surface of ZnSe IRE while the angle of incidence was varied from 45° to 60° with a 5° interval. The normalized ATR spectra of Teflon/

polyimide/Teflon film acquired by increasing the incident angles are shown in Figure 4.18. All ATR spectra only reveal the chemical absorption bands at 1201 and 1146 cm^{-1} which assigned for Teflon. The acquired spectra indicate that no spectral change was detected. Since the probing depth was limited within the order of few micrometers away from the IRE/sample interface, the observed spectra information is dominated by that at the surface. As a result, the depth dependent chemical information of the constituent part of multilayered film cannot be detected.

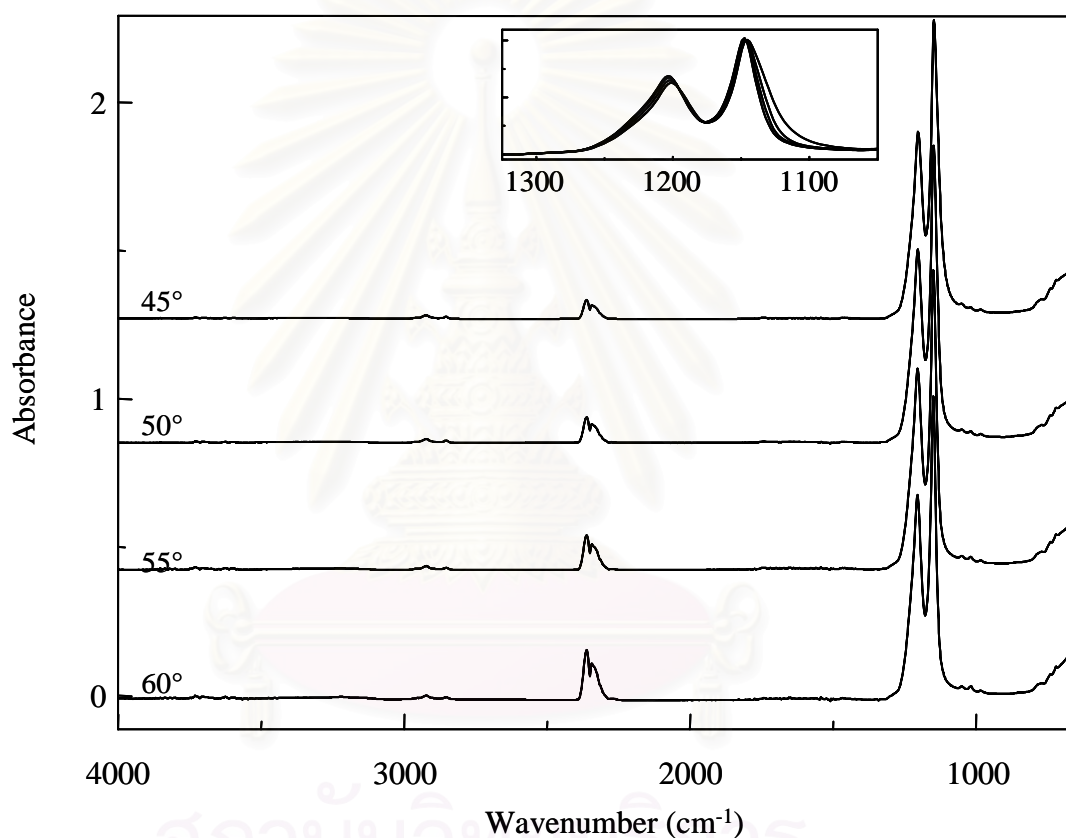


Figure 4.18 Normalized ATR spectra of Teflon/Polyimide/Teflon acquired by conventional ATR using ZnSe IRE. The angle of incidence was varied from 45° to 60° with a 5° interval.

4.5.2.2 Diamond μ ATR sensor

Diamond IRE can penetrate into the film by pressing the film against the diamond. By performing controlled diamond penetration and/or illuminating the sampling area with various aperture size of the infrared microscope, the spectral feature of a specific layer at a certain distance from the surface can be selectively collected. Based on the brilliant cut shape of diamond IRE and the experimental operation, depth dependent analysis by the novel diamond IRE can be divided into two modes: (1) varying diamond penetration under constant aperture (2) varying aperture under constant diamond penetration.

Varying diamond penetration under constant aperture

For depth profiling of multilayered film by the diamond μ ATR sensor, Teflon/polyimide/Teflon film was brought into contact with the culet of diamond IRE by applied pressure. The diamond tip (the culet and a portion of pavilion facet of diamond IRE) was penetrated into the specimen by the increasing applied pressure. The normalized ATR spectra of Teflon/polyimide/Teflon film by varying the diamond penetration under fixed aperture size are shown in Figure 4.19B. The spectral feature at a greater depth can be acquired by pressing the diamond tip to a greater sampling depth. At the lowest applied pressure, the characteristic absorption bands appeared at 1201 and 1146 cm^{-1} . These spectral feature and band position are similar to the surface spectrum of Teflon that taken with the conventional ZnSe IRE (Figure 4.19A). At the deeper diamond penetration, the absorption magnitudes of Teflon increase with the increased sampling depth. At the higher applied pressure, the absorption magnitudes of Teflon decrease while the new bands appear. The appearances of the new bands reveal the spectral feature of polyimide that confirmed by the same spectral feature of polyimide acquired by the conventional ATR technique. In case of the highest applied pressure, the observed spectra suggested that the diamond tip was not penetrated into another Teflon layer but punch through polyimide film. Since polyimide is hard and rigid material, the spectral changing associated with the layer beyond the layer of polyimide was not detected.

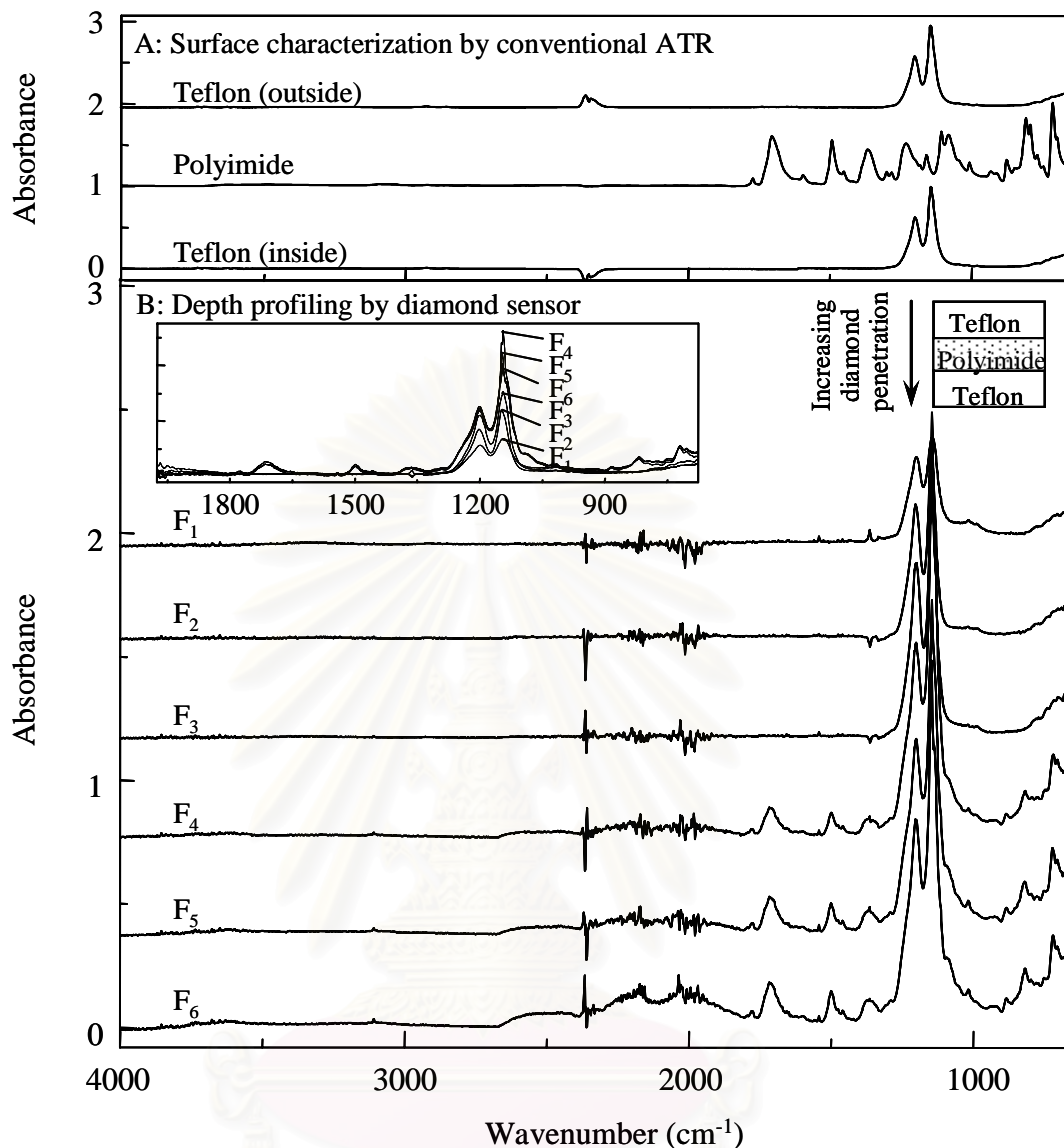


Figure 4.19 Normalized ATR spectra of multilayer film: (A) spectra of Teflon (outside), polyimide, and Teflon (inside) acquired by the conventional ATR and (B) depth profiling of Teflon/Polyimide/Teflon by increasing diamond penetration under a constant aperture of the diamond μ ATR sensor, F_i denote the applied force that $F_1 < F_2 < F_3 < F_4 < F_5$.

Constant diamond penetration with varying aperture

Depth profiling of the same specimen using the diamond μ ATR sensor was performed by varying the sizes of aperture under the fixation of the diamond penetration as shown in Figure 4.20B. The diamond IRE was penetrated into the Teflon/polyimide/Teflon film while the aperture of the infrared microscope was set at 500x500, 400x400, 300x300, 200x200 and 100x100 μm^2 . If a small aperture was employed, the observed spectra show the lower absorption intensity of Teflon and higher intensity of polyimide. This indicated that the diamond tip is penetrated into the interface between Teflon and polyimide. If the larger aperture were employed, the absorption intensity of Teflon increases while the intensity of polyimide decreases as thickness of sampling increase. The spectral information of thicker film were acquired, the sampling depth is covered higher Teflon/polyimide ratio. This ratio suggests that polyimide is a hard and rigid material, the diamond tip penetrates into the interface between Teflon (first layer) and polyimide film.

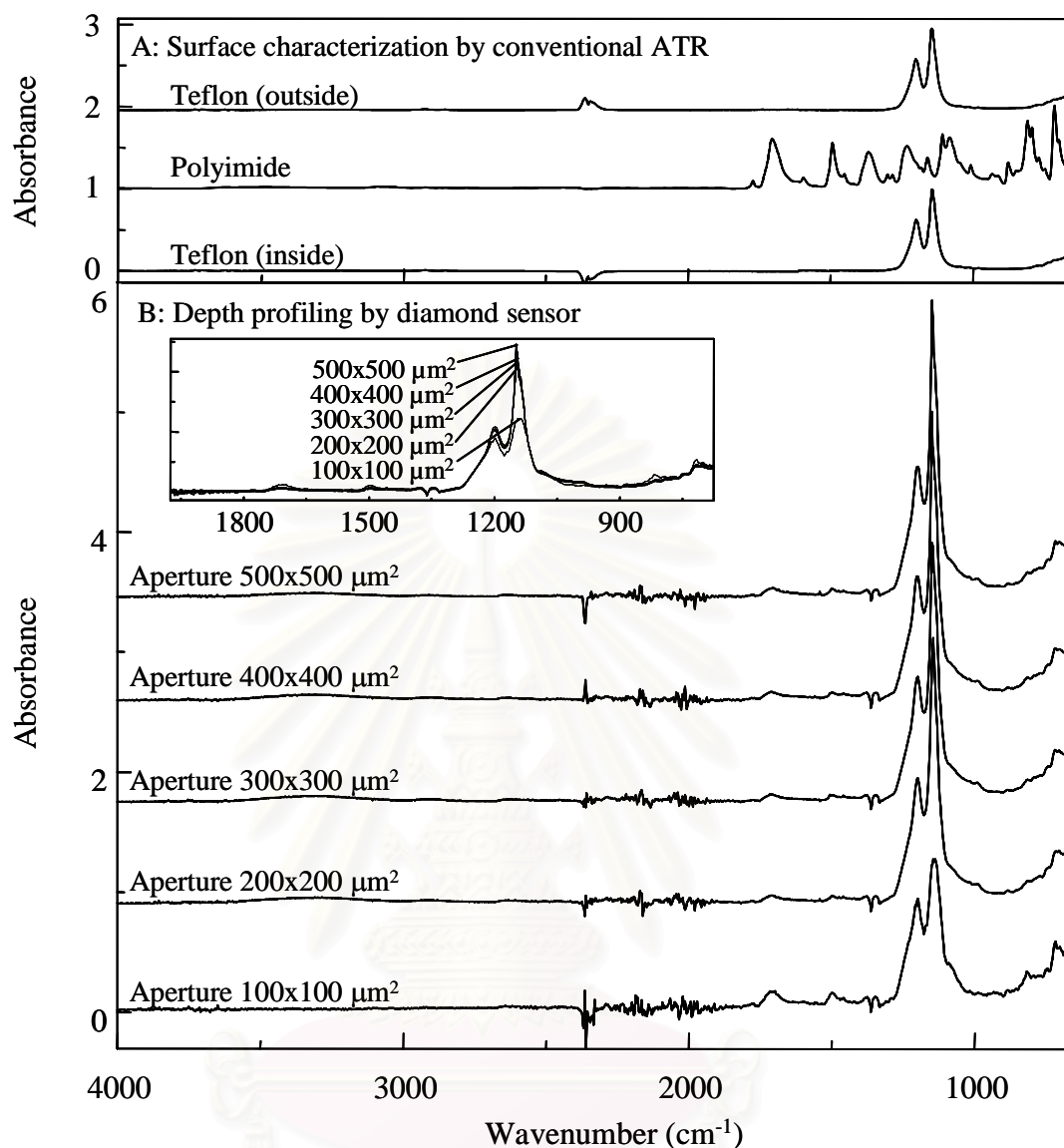


Figure 4.20 ATR spectra of multilayered film: (A) spectrum of each layers of Teflon/Polyimide/Teflon acquired by conventional ATR and (B) depth profiling of Teflon/Polyimide/Teflon by increasing aperture under a constant diamond penetration of the diamond μ ATR sensor.

By comparing the conventional ATR with diamond μ ATR techniques, the effect of depth dependent analysis of multilayered film was investigated. The components of multilayered film are three layers including Teflon, polyimide, and Teflon respectively. For the diamond μ ATR experiments, the depth profiling was analyzed by varying diamond penetration and aperture. These operations can detected the spectral change from that of the Teflon in first layer to that of the polyimide in second layer. However due to the rigidity of second layer, the diamond

tip can not have sufficient contact with the third layer. As a result, the spectral of Teflon in third layer was not detected. In the case of conventional ATR technique, the acquired spectra by varying the incident angle (Figure 4.18) only reveal the chemical species of Teflon in the first layer. The characteristic spectral features suggested that the conventional ATR technique cannot detect the depth dependent composition of the too thick multilayered film (*i.e.*, thicker than 5 μm). The novel diamond μATR sensor can be employed for depth profiling purpose where the chemical information beyond the surface of solid sample can be selectively acquired.



สถาบันวิทยบริการ
จุฬาลงกรณ์มหาวิทยาลัย

CHAPTER V

CONCLUSIONS

Novel internal reflection elements (IRE) made of a gem quality round brilliant cut natural diamonds was employed for ATR FT-IR spectral acquisition using an infrared microscope. The technique takes advantage of the total internal reflection phenomenon at the pavilion facet of the faceted diamond. The evanescent field generated at the interface can be employed for spectral acquisition of a material attached to the pavilion facet of the diamond. A good contact between the diamond IRE and the hard and rigid solid samples can always be achieved simply by pressing the specimen against the inherently hardest diamond. The major drawbacks of the ATR FT-IR technique associated with the degree contact were eliminated while the strong evanescent field was exploited. By the sharp-tip configurations of diamond IRE, surface, bulk, and/or depth-dependent information of the solid materials can be acquired. The study of surface characterization and depth profiling of the identical sample was demonstrated in order to compare between ATR FT-IR spectra acquired by the novel IRE and those by conventional zinc selenide IRE.

Regarding the surface characterization of liquid and solid samples, the chemical information obtained from the diamond μ ATR sensor is similar to those from the conventional ATR IRE. However, the relative intensity of ATR spectra acquired by diamond sensor is greater than that of conventional ATR IRE due to the nature of the incident radiation penetrating into the sample.

Because of small penetration depth of conventional ATR technique, the depth profiling of a multilayered film cannot be performed via conventional IRE while it can be accomplished by the sharp-tip diamond IRE. By controlling penetration of the diamond IRE through the sample and/or illuminating the pavilion facet with various aperture sizes of the couple radiation, the spectral information of a specific layer at a certain distance from the surface can be selectively collected.

REFERENCES

1. Stevens, M.P. (Ed.), Polymer Chemistry, pp. 130-149. New York: Oxford University Press, 1999.
2. Shaojin, J., Pingkai, J.; Zhicheng, Z.; and Zhongguang, W. Effect of Carbon-black Treatment by Radiation Emulsion Polymerization on Temperature Dependence of Resistivity of Carbon-black-filled Polymer Blends. Radiat. Phys. Chem. 75 (2006): 524-531.
3. Smith, B. C. Fundamentals of Fourier Transform Infrared Spectroscopy. New York: CRC Press, (1996).
4. Kumar, A.; Commereuc, S.; Gonon, L.; and Verney, V. Depth-profile of Photo-oxidation of Polyoctenamer. Polym. Degrad. Stab. 75 (2002): 509-516.
5. Chalmers, J. M., and Griffiths, P. R. (Eds). Handbook of Vibrational Spectroscopy volume 2. UK: John Wiley & Sons Ltd, 2002.
6. Urban, M. W. (ed.) Attenuated Total Reflectance Spectroscopy of Polymer: Theory and Practice, Washington, DC: American Chemical Society, 1996.
7. Harrick, N. J. (ed.), Internal Reflection Spectroscopy. New York: Harrick Scientific Corporation, 1979.
8. Huang, J.; and Urban, M. W. Novel Approach to Quantitative Depth Profiling of Surfaces using ATR/FT-IR Measurements. Appl. Spectrosc. 47 (1993): 973-981.
9. Buffeteau, T.; Desbat, B.; and Eyquem. D. Attenuated total reflection Fourier Transform Infrared Microspectroscopy: Theory and Application to Polymer Samples. Vib. Spectrosc. 11 (1996): 29-36.
10. Padermshoke, A.; Katsumoto, Y.; Sato, H.; Ekgasit, S.; Noda, I.; and Ozaki, Y. Surface Melting and Crystallization Behavior of Polyhydroxyalkanoates Studied by Attenuated Total Reflection Infrared Spectroscopy. Polymer 45 (2004): 6547-6554.
11. Asahara, J.; Takemura, A.; Hori, N.; Ono, H.; and Matsui, H. Crosslinked Acrylic Pressure Sensitive Adhesives. 3. Effect of Adhered on Film Formation. Polymer 45 (2004): 4917-4924.

12. Nagai, N.; Matsunobe, T.; and Imai, T. Infrared Analysis of Depth Profiles in UV-photochemical Degradation of Polymers. Polym. Degrad. Stab. 88 (2005): 224-233.
13. Nagai, N.; Okumura, H.; Imai, T.; and Nishiyama, I. Depth Profile Analysis of the Photochemical Degradation of Polycarbonate by Infrared Spectroscopy. Polym. Degrad. Stab. 81 (2003): 491-496.
14. Vreugdenhil, A. J.; Donley, M. S.; Grebasch, N. T.; and Passinault, R. J. Applications of Vibrational Spectroscopy to the Analysis of Novel Coatings. Prog. Org. Coat. 41 (2001): 254-260.
15. Ekgasit, S.; and Ishida, H. Optical Depth Profiling by Attenuated Total Reflection Fourier Transform Infrared Spectroscopy Using an Incident Beam with Arbitrary Degree of Polarization. Vib. Spectrosc., 13 (1996): 1-9.
16. Ferraro, J. R.; and Valkenburg, E. Organics of the Diamond Anvil Cell. Spectroscopy 14 (1999): 19-23.
17. Katon, J. E. Infrared Microspectroscopy: a Review of Fundamentals and Applications. Micron 27 (1996): 303-314.
18. Wilhelm, P. Application of FT-IR Microscopy with Materials Analysis. Micron 27 (1996): 341-344.
19. Thommasson, J.; Coin, C., Kahraman, H.; and Fredericks, P. M. Attenuated Total Reflectance Infrared Microspectroscopy of Coal. Fuel 79 (2000): 685-691.
20. Scherzer, T. Depth Profiling of the Conversion during the Photopolymerization of Acrylates Using Real-time FTIR-ATR Spectroscopy. Vib. Spectrosc. 29 (2002): 139-145.
21. Ekgasit, S.; and Thongnopkun, P. Novel Attenuated Total Reflection Fourier Transform Infrared Microscopy Using a Gem Quality Diamond as an Internal Reflection Element. Appl. Spectrosc. 59 (2005): 1-6.
22. Ekgasit, S.; and Padermshoke, A. Optical Contact in ATR FT-IR Spectroscopy. Appl. Spectrosc. 55 (2001): 1352-1359.
23. Ekgasit, S.; and Thongnopkun, P. Transflectance Spectra of Faceted Diamonds Acquired by Infrared Microscopy. Appl. Spectrosc. 59 (2005): 108-113.



APPENDICES

สถาบันวิทยบริการ
จุฬาลงกรณ์มหาวิทยาลัย

APPENDICES

1. Homemade diamond μ ATR accessory



Figure 1 Composition of homemade accessory for diamond probing head.

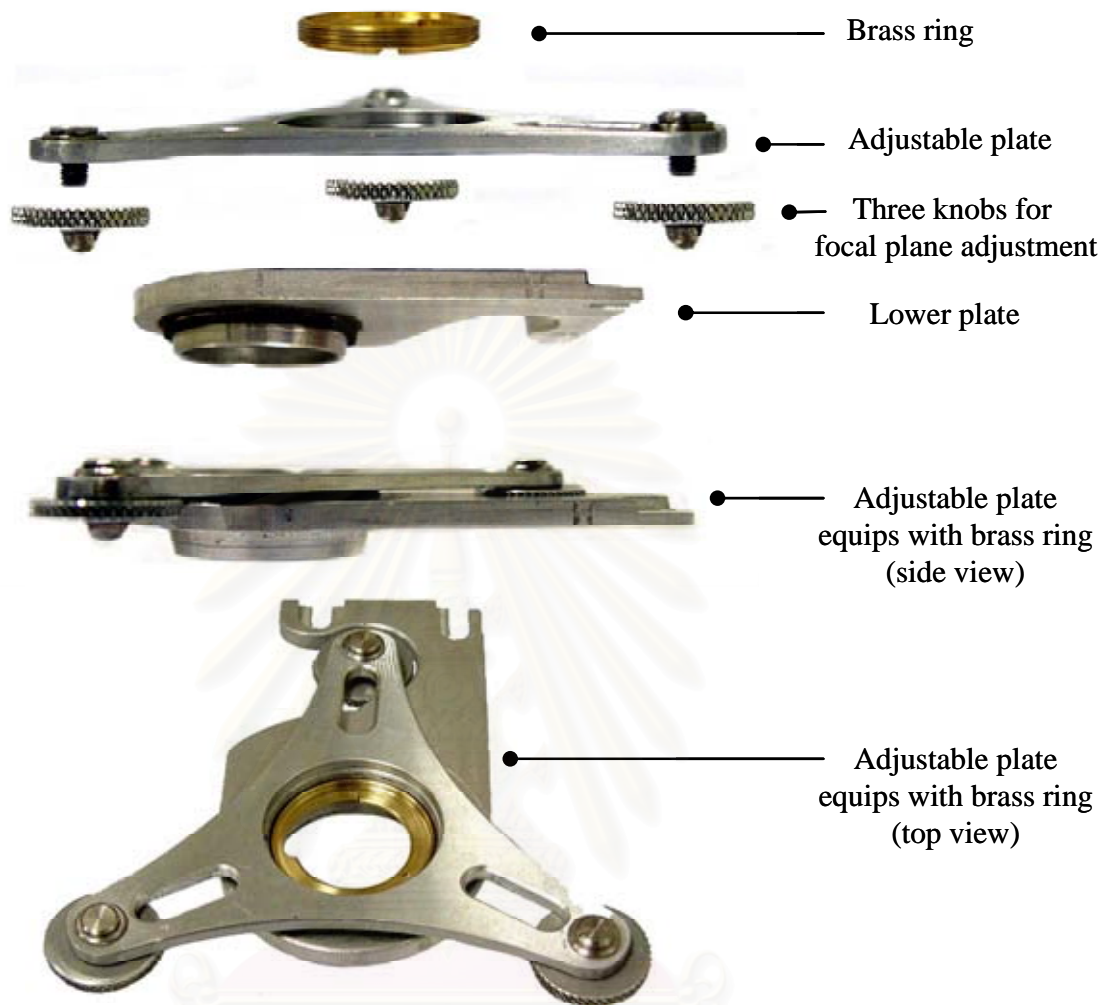


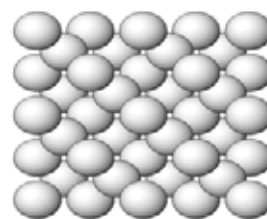
Figure 2 Composition of the homemade accessory for adjustable reflection plane.

สถาบันวิทยบริการ
จุฬาลงกรณ์มหาวิทยาลัย

2. Chemical and physical properties of diamond



A



B

Figure 3 Diamond (A) and crystal structure (B)

Chemical composition	Carbon (C)
Hardness	10
Refractive index	2.417 (dispersion: 0.044)
Specific Gravity	3.515
Color	variable
Crystal System	isometric; $4/m\bar{3}2/m$
Transparency	transparent to translucent in rough crystals
Heat sensitivity	No
Luster	adamantine to waxy
Cleavage	perfect in 4 directions

สถาบันวิทยบริการ
จุฬาลงกรณ์มหาวิทยาลัย

3. Peak assignments

Table 1 Peak assignments of mineral oil.

Wavenumber (cm ⁻¹)	Peak Assignment
2910, 2845	C-H stretching
1463	-(CH ₂)- bending
720	CH ₂ rocking

Table 2 Peak assignments of PVC

Wavenumber (cm ⁻¹)	Peak Assignment
2952, 2922, 2867	C-H stretching
1731	C=O stretching of plasticizer
1427, 1377	CH ₂ bending
1038	C-O stretching of plasticizer
690	C-Cl stretching

Table 3 Peak assignments of OPP/PE bi-layered film.

Wavenumber (cm ⁻¹)	Peak Assignment
<u>OPP</u>	
2952	Asymmetric C-H stretching, -CH ₃
2915	Asymmetric C-H stretching, -CH ₂
2866	Symmetric C-H stretching, -CH ₃
2833	Symmetric C-H stretching, -CH ₂
1455	CH ₃ bending
1375	CH ₃ bending
1165	C-C stretching
970	CH ₃ rocking
<u>PE</u>	
2910	Asymmetric C-H stretching, -CH ₂
2845	Symmetric C-H stretching, -CH ₂
1463	-(CH ₂)- bending
720	CH ₂ rocking

Table 4 Peak assignments of Teflon/Polyimide/Teflon multilayered film.

Wavenumber (cm ⁻¹)	Peak Assignment
<u>Teflon</u>	
1201, 1146	C-F stretching
<u>Polyimide</u>	
1774, 1714	C=O stretching of imide ring
1600, 1597	C-H stretching of aromatic ring
1390	C-N stretching of imide ring
1260	C-O-C stretching
722	C-H bending of aromatic ring

CURRICULUM VITAE

Wipaporn Akkarayanyong

- 1982 Born : February, 23rd in Bangkok, Thailand
Father : Mr. Wichan Akkarayanyong
Mother : Mrs. Yaovapa Akkarayanyong
- 1988 Elementary School (Sakunsuksa School, Nakornratchasima)
- 1994 Primary School (Sakunsuksa School, Nakornratchasima)
- 2000 High School (Pakchong School, Nakornratchasima)
- 2004 Bachelor of Science (Chemistry),
Kasetsart University, Bangkok
- 2006 Master of Science (Petrochemistry and Polymer Science),
Chulalongkorn University, Bangkok

สถาบันวิทยบริการ
จุฬาลงกรณ์มหาวิทยาลัย